國立臺灣大學電機資訊學院光電工程學研究所

碩士論文

Graduate Institute of Photonics and Optoelectronics
College of Electrical Engineering and Computer Science
National Taiwan University

Master Thesis

應用於折射率感測的穩定封裝之微光纖線圈共振腔與其長時間穩定性提升

A Stable Packaged Microfiber Coil Resonator for Refractive Index Sensing and Its Long-term Stability Improvement

呂宣毅

Xuan-Yi Lu

指導教授：王倫 博士

Advisor: Lon A. Wang, Ph.D.

中華民國 106 年 3 月

March, 2017

doi:10.6342/NTU201700769

國立臺灣大學碩士學位論文
口試委員會審定書

應用於折射率感測的穩定封裝之
微光纖線圈共振腔與其長時穩定性提升
A Stable Packaged Microfiber Coil Resonator for Refractive Index Sensing and Its Long-term Stability Improvement

本論文係呂宣毅君（學號 R02941002）在國立臺灣大學光電工程學研究所完成之碩士學位論文，於民國 106 年 3 月 31 日承下列考試委員審查通過及口試及格，特此證明

口試委員：

王倫 （指導教授）

廖顯奎　　劉文豐

黃念祖

所　長　林恭如

誌謝

能完成這本論文與碩士學業，首先必須要感謝我的父母親，從小到大我的父母總是為了我不辭辛勞地打理我生活上的大小事，讓我能無後顧之憂地專心於課業學習與實驗研究，感謝你們的付出和支持。同時，我也要感謝王倫老師的指導，不僅是實驗上的建議與鼓勵包括了人生態度與對未來生涯的建議，我都會謹記在心。

感謝宗翰學長讓我有機會可以一探微光纖共振腔這個領域。在進來研究所前我從未想過原來光纖可以做得僅有數個微米，也沒想過自己有朝一日居然能夠操控這麼纖細的微光纖來進行研究。學長的指導和傳承下來的研究設備是這個研究的基石。

感謝實驗室的學長們：建宏、方向、智昇、哲安、志豪、耀宇、彥博、偉弘，謝謝你們帶領我認識這個實驗室。或許研究的領域各不相同，但是當我請教學長們問題時，學長們也是盡可能地幫忙我。和學長們相處，讓我感覺實驗室就像是個大家庭一樣。相信這樣的氣氛會在我們實驗室不斷延續下去。

感謝惟中、永泰、世昌、昇宏。在這個碩士班過程有幸認識你們，和你們一起歡笑、一起難過、一起努力。大家互相鼓勵、彼此切磋，這些都是能夠讓研究能夠繼續向前的原因之一。

感謝世昕、健甫、冠宏、建霖。謝謝你們幫忙這個有時表現落漆的學長，給我研究上的幫助與建議，這些我都銘記在心。

在研究所的這段時間，仔細想想要感謝的人還有很多，應力所育文學長、生醫電子所的筌凱和柏承、機械工廠的師傅們… …等等，感謝老天爺讓我能夠與這麼多人結緣。我不是一個太會說話的人，想不出什麼美麗的詞藻來表達對所有人的感謝之情。在此只能用簡單一句話來作結，謝謝大家。

doi:10.6342/NTU201700769

中文摘要

近來，微光纖線圈共振腔在非線性光學和光纖感測吸引許多目光。和以半導體製作的微共振腔相比，微光纖線圈共振腔擁有例如低傳輸損耗，容易和一般光纖元件結合等特點。透過增加線圈數或堆疊線圈，微光纖線圈共振腔可以達到相當高的品質因子。然而，沒有保護的微光纖線圈共振腔很容易受到外界環境干擾，限制了微光纖線圈共振腔的應用。因此，微光纖線圈共振腔的保護方法是本篇論文的主要焦點。

在此論文中，首先我們介紹微光纖線圈共振腔的製作過程和保護方法。我們利用改良的小型光纖抽絲塔，以氫氧焰作為熱源製作直徑 3 微米的微光纖。接著我們展示微光纖線圈共振腔的製作架構。透過具有超長工作距離的物鏡和 CCD 元件，我們可以即時觀測繞線過程，有助於儘早檢測出錯誤。具有良好同心度和穩定性的繞線系統使我們可以準確地控制微光纖線圈共振腔每圈的間隔。我們使用以正己烷稀釋過的聚二甲基矽氧烷作為微光纖線圈共振腔的包裝材料。稀釋過的聚二甲基矽氧烷擁有較低的黏滯性，方便在繞線過程中調整線圈。以此方法製作的微光纖線圈共振腔品質因子可以達到 5×10^5，而且頻譜表現可以維持 5 天。

接著我們嘗試以聚二甲基矽氧烷包裝之微光纖線圈共振腔進行折射率感測。將微光纖線圈共振腔放置在一壓克力架構中，並以葡萄糖水溶液作為折射率變化。微光纖線圈共振腔的偵測極限為 7×10^{-4}。為了增加微光纖線圈共振腔應用的潛力，我們將剩餘微光纖部分以紫外光固化膠覆蓋，進一步提升微光纖線圈共振腔的穩定性。如此微光纖線圈共振腔的表現可以維持長達一個月沒有明顯劣化。

關鍵字：微光纖、微光纖線圈共振腔、高品質因子、折射率感測、微光纖封裝方法

doi:10.6342/NTU201700769

Abstract

Recently, microfiber coil resonators (MCR) have attracted much attention in nonlinear optics and optical sensing. Compared with the semiconductor based micro resonators, MCRs have attractive properties such as low propagation loss and easy connection with conventional optical fiber devices through their tapered sections. Moreover, by increasing coil turns or stacking microfiber turns, MCRs can achieve very high quality factor. However, an unpackaged MCR is easily affected by surrounding disturbance, which limits its applications. Therefore the methods to protect MCRs is the main focus of this work.

In this work, we firstly introduce fabrication process and protection method of MCR. A 3-μm diameter microfiber was produced by using a modified miniature fiber drawing tower. The hydrogen oxygen flame was applied as heat source. Then the experimental setup for fabricating MCR is demonstrated. With the extra long working distance objective and CCD, the coiling process could be observed *in situ*. This helps us early detect the faults during coiling process. The coiling system with good concentricity and stability helps us control the microfiber coil accurately. Polydimethylsiloxane (PDMS) diluted with hexane was used as package material for MCR. Hexane-diluted PDMS has lower viscosity so the microfiber coil could be turned

doi:10.6342/NTU201700769

around easily. The quality factor of PDMS-packaged MCR was 5 x 10^5 and could maintain for 5 days.

Next, we tried to use PDMS-packaged MCR as refractive index sensor. PDMS-packaged MCR was put in a PMMA structure and glucose solutions were used for different refractive index. The detection limit of PDMS-packaged MCR was about 7×10^{-4} RIU. To increase the potential of practical applications, long-term stability of MCR was further improved by protecting microfibers with UV glue. The performance of MCR could maintain over a month without degradation.

Key words: microfiber, microfiber coil resonator, high quality factor, refractive index sensing, microfiber package method

doi:10.6342/NTU201700769

Statement of Contribution

1. Develop the package method for microfiber coil resonator and improve the long-term stability. The result had been poster presented in *MOC 2015*.
2. Cooperate with the group of Prof. A. B. Wang in NTU to fabricate micro-two-phase flow detection by microfibers in microfluidic chip. The result had been published on the journal *Sensors and Actuators B: Chemical* 2016.

doi:10.6342/NTU201700769

CONTENT

誌謝 ..... **i**

中文摘要 ..... **ii**

Abstract ..... **iii**

Statement of Contribution ..... **v**

CONTENT ..... **vi**

LIST OF FIGURES ..... **viii**

LIST OF TABLES ..... **xi**

LIST OF ABBREVIATIONS ..... **xii**

Chapter 1 Introduction **1**

1.1 Motivation 1

1.2 Literature Review 5

1.2.1 Microfiber Resonator-based Sensors 5

1.2.2 Package Materials of Microfiber Device 6

1.3 Theory of MCRs 8

1.4 Organization of the Thesis 14

Chapter 2 Fabrication and Optical Characteristics of PDMS-packaged MCRs **15**

2.1 Fabrication of PDMS-packaged MCRs 15

2.2 Optical Characteristics of PDMS-packaged MCRs 23

Chapter 3 Refractive Index Sensing and Long-term Stability Improvement **27**

doi:10.6342/NTU201700769

3.1 Experimental Setup of Refractive Index Sensing 27
3.2 Measurement Results and Discussion 33
3.3 Long-term Stability Improvement 43

Chapter 4 Conclusions and Future Work 50

References 52

doi:10.6342/NTU201700769

LIST OF FIGURES

Fig. 1-1 A schematic diagram of single layer MCR.....4

Fig. 1-2 A schematic diagram of MCR. 13

Fig. 2–1 Photograph of modified miniature fiber drawing tower. 16

Fig. 2-2 (a) Schematic setup for fabrication of MCRs.....19

Fig. 2-2 (b) Photograph of the fabrication system. 20

Fig. 2-3 Top view of V-shaped groove carved on the Teflon bar. 21

Fig. 2-4 Photograph of bevel of Teflon bar……21

Fig. 2-5 Photograph of a bare MCR after ethanol was dropped on it. 22

Fig. 2-6 Photograph of PDMS-packaged MCR with 3 turns. 22

Fig. 2-7 Transmission spectra of MCR before (blue line) and after (red line) curing. 24

Fig. 2-8 (a) Transmission spectrum of PDMS-packaged MCR and (b) one resonant dip and its Lorentz curve fitting…… 25

Fig. 2-9 Power evolutions of a bare and a PDMS-packaged MCRs over 5 days measured in 1550 nm wavelength…… .....……26

Fig. 2-10 Transmission spectra of simulation (red line) and PDMS-packaged MCR (blue line)…….. 26

Fig. 3-1 Photograph of 4-layer PMMA structure and MCR clip. 29

doi:10.6342/NTU201700769

Fig. 3-2 Dimensions of four PMMA plates for PMMA structure. 30

Fig. 3-3 (a) Photograph of PDMS-packaged MCR in PMMA structure. (b) Close-up Photo of PDMS coating zone and RI sensing region. 31

Fig. 3-4 Photograph of a PDMS-packaged MCR during RI sensing. 32

Fig. 3-5 Transmission spectrum of PDMS-packaged MCR before RI sensing. 36

Fig. 3-6 (a)-(e) Measured transmission spectra of PDMS-packaged MCR in each glucose solutions of first measurement. (f) The shifts of the resonant dip in the transmission spectra……..……37

Fig. 3-7 (a)-(e) Measured transmission spectra of PDMS-packaged MCR in each glucose solutions of second measurement. (f) The shifts of the resonant dip in the transmission spectra……..……38

Fig. 3-8 (a)-(e) Measured transmission spectra of PDMS-packaged MCR in each glucose solutions of third measurement. (f) The shifts of the resonant dip in the transmission spectra……..……39

Fig. 3-9 Dependence of the measured wavelength shifts on the refractive index of glucose solutions and its linear fit to the data ……..... 40

Fig. 3-10 Microscopic image of microfiber in the RI sensing region after RI sensing... 40

Fig. 3-11 Photograph of microfibers after they were immersed in 30% glucose solution and deionized water……..41

doi:10.6342/NTU201700769

Fig. 3-12 Transmission spectra of PDMS-packaged MCR before and after RI sensing……41

Fig. 3-13 Lorentz curve fittings of (a) dip A and (b) dip B. 42

Fig. 3-14 Photograph of U-shaped Aluminum and MCR clip. 46

Fig. 3-15 Photograph of package system. 46

Fig. 3-16 Photograph of microfiber in PDMS with micro-bending.....47

Fig. 3-17 Photograph of PDMS-packaged MCR on UV glue coating substrate. 47

Fig. 3-18 (a) Transmission spectrum of PDMS-packaged MCR and (b) one resonant dip and its Lorentz curve fitting…….....48

Fig. 3-19 Transmission spectra of the original PDMS-packaged MCR with protection and the same one after one month…….....49

doi:10.6342/NTU201700769

LIST OF TABLES

Table 3-1 Refractive indices for the glucose solutions with different concentrations. ……31

Table 3-2 Values, averages and standard deviations of wavelength shift at different glucose solutions. ……36

doi:10.6342/NTU201700769

LIST OF ABBREVIATIONS

MCR	Microfiber coil resonator
PDMS	Polydimethylsiloxane
FSR	Free spectral range
FWHM	Full width at half maximum
CCD	Charge-coupled Device
PMMA	Polymethylmethacrylate
PE	Polyethylene

doi:10.6342/NTU201700769

Chapter 1 Introduction

1.1 Motivation

Since the prediction of their low losses by Kao and Hockham [1], optical fibers have been developed for enormous applications comprising the fields of telecommunications [2], lasers [3], gratings [4], and sensors [5], etc. Compared with electrical wires, optical fibers have the advantages of extremely high bandwidth and large data carrying capacity, low loss for long distance transmission, no crosstalk and low bit error rates, immunity to electromagnetic interference, difficult to eavesdrop for signal security, small size and low weight, and so on. Other than the above-mentioned advantages for telecommunication, fiber optic components also benefit from those characteristics and therefore we can produce many useful devices such as polarizers, couplers, isolators, circulators, filters, interferometers, modulators and amplifiers [6, 7]. These devices form the physical layer of an optical distribution network, an important sector for the Internet.

Contrary to using optical fiber in telecommunication, the use of optical fiber in the scale of several micrometers is much struggled. When the optical fibers were used as components or sensors, sometimes they needed to be bent for more efficient

doi:10.6342/NTU201700769

performance. However, the diameter of optical fiber (typically 125 μm) is limited to the minimal bending radius. A single-mode bend optimized fiber can be bent down to radius of curvature of 12 mm with low loss and long lifetime [8]. Bending radius smaller than 10 mm will increase the loss and the fiber would be easily broken [9]. Microfiber is therefore an interesting research topic to solve the problem that conventional optical fiber cannot achieve. Its diameter ranges from tens of nanometers to several micrometers. Most of the optical fiber components can be miniaturized by replacing optical fibers to microfibers. The dimension of microfiber makes it much suitable to be a sensor due to its large evanescent field, which improves sensitivity. A large evanescent field will propagate in the surface of microfiber which strongly interacts with the environment.

Recently, microfiber coil resonators (MCR) have attracted much attention in nonlinear optics [10] and optical sensing [11-13]. An MCR is usually fabricated by coiling a microfiber on a rod, and its resonance is caused by optical coupling of the evanescent field of adjacent microfibers. A schematic diagram of MCR is shown in Fig. 1-1. Compared with the semiconductor based micro resonators, MCRs have attractive properties such as low propagation loss and easy connection with conventional optical fiber devices through their tapered sections. Moreover, by increasing coil turns [14] or stacking microfiber turns [15], MCRs can achieve very high quality factor. However,

doi:10.6342/NTU201700769

an unpackaged MCR is easily affected by surrounding disturbance, which limits its applications. Therefore it is very important to find methods to protect MCRs. Some low refractive index materials, such as Teflon AF (amorphous fluoroplastics) [16] and UV glues [17], have been used to package MCRs. Depending on the type of Teflon AF, the typical molding temperature is 240℃ or higher. For fully curing, UV glues need high power UV light source.

In this thesis, we will introduce a low cost and easy alternative which use polydimethylsiloxane (PDMS) to package MCR. The optical characteristics and refractive index sensitivity of PDMS-packaged MCR were measured. To further improve the stability of whole structure, the rest of microfiber was covered with UV glue.

doi:10.6342/NTU201700769

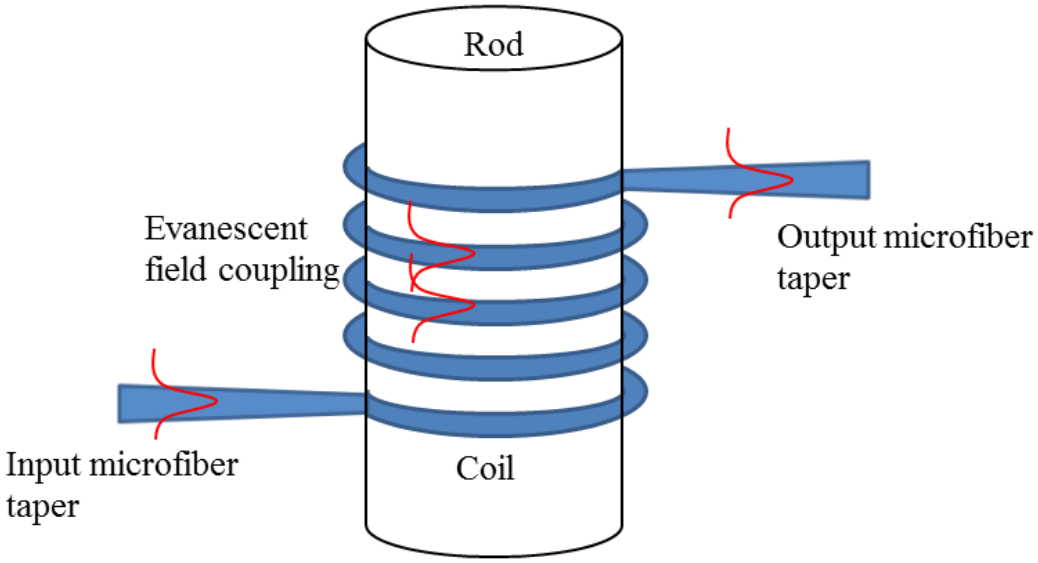

Fig. 1-1 A schematic diagram of single layer MCR.

doi:10.6342/NTU201700769

1.2 Literature Review

Microfibers have been studied for a decade [18-21] and it can still be regarded as an important topic. The research of microfibers mainly focused on the fabrication methods, microfiber-based devices, sensor applications, nonlinearity, etc. Several groups started the research and more and more researchers have been involved in recent years. Here are the significant results of these research groups listed thereinafter.

1.2.1 Microfiber Resonator-based Sensors

There are three types of microfiber resonators, namely loop, knot and coil resonators. For sensing applications, microfiber resonators can provide high sensitivity, low detection limits due to high quality factors, and good wavelength selectivity due to small resonant bandwidths.

Sensors based on microfiber resonators have been investigated for different applications, for example, they could serve as refractive index sensors [22-26], temperature sensors [24, 27], current sensors [28-31], humidity sensors [32-34], chemical sensors [35], gas sensors [36], and magnetic field sensors [37, 38]. Most of them are based on refractive index detection because of large evanescent field outside the microfiber which makes it easy to detect the variation of surrounding refractive index. The refractive index change will change the loss or resonant dip of light spectrum

doi:10.6342/NTU201700769

in microfiber resonators. The thermal expansion coefficient and thermal optic coefficient of silica are lower. To be a temperature sensor, microfiber resonator should be embedded in polymer with high thermo-optic coefficient. The working principle of current sensor is similar to temperature sensor. Heat generated from electrical current results in thermo-optic effect and thermal expansion effect, which make resonant dip shift. As a humidity sensor, the microfiber resonators should be coated with polymer materials with high humid sensitivity [32, 34] or alternatively using polymer microfiber [33]. As the same concept, microfiber resonator could be a gas sensor if coated with materials sensitive to specific gas. For instance, microfiber knot resonator coated with Pd layer would be sensitive to hydrogen concentration [36]. The magnetic field sensor is based on refractive index change. Microfiber knot resonator is immersed in a magnetic fluid, and under applied magnetic field, the refractive index of magnetic fluid will be changed, which induces resonant dip shift.

1.2.2 Package Materials of Microfiber Device

The environment will severely affect the loss of microfiber. Particle would adhere to microfiber, which increases the scattering loss. The hydroxyl bonds would generate to increase the loss of microfibers under humid condition. Besides, the microfiber

doi:10.6342/NTU201700769

structure is vulnerable to surrounding disturbance. Therefore, it is necessary to package microfiber devices to maintain their performance. Basically, the materials used to package microfiber devices should have low refractive index. Some low refractive index materials have been used, such as Teflon AF [16], UV glue [17], and aerogel [39]. Some materials could not only protect microfiber devices but also improve the performance of devices. Hernández-Romano *et. al.* packaged their microfiber-based temperature sensor by covering PDMS because of its high thermo-optic coefficient [40]. Cham *et. al.* used microfiber knot resonator coated with polyaniline as an alcohol concentration sensor since polyaniline could generate chemical bond with alcohol [35].

doi:10.6342/NTU201700769

1.3 Theory of MCRs

Microfiber coil resonator is the most complex and also the only 3-dimentional microfiber-based resonator among other types of microfiber resonators. Its unique 3-dimensional structure provides several special applications [41]. In this section, we will study the theory of the MCR.

The transmission properties of MCR can be expressed by using coupled mode equations [42]. An MCR consisting of M turns of microfiber is shown in Fig. 1-2. Assume the coupling between non-adjacent turns can be ignored. The corresponding light field amplitude of the m-th turn is $A_m(s)$ which satisfies the set of following equations [43].

doi:10.6342/NTU201700769

$$-\frac{d}{ds}\begin{pmatrix} A_1(s) \\ A_2(s) \\ \vdots \\ A_m(s) \\ \vdots \\ A_{M-1}(s) \\ A_M(s) \end{pmatrix} = i\begin{pmatrix} 0 & \kappa_{12}(s) & 0 & \cdots \\ \kappa_{21}(s) & 0 & \kappa_{23}(s) & \cdots \\ 0 & \kappa_{32}(s) & 0 & \cdots \\ \vdots & \vdots & \vdots & \cdots \\ 0 & 0 & 0 & \cdots \\ 0 & 0 & 0 & \cdots \\ 0 & 0 & 0 & \cdots \end{pmatrix}$$

$$\begin{pmatrix} 0 & 0 & 0 \\ 0 & 0 & 0 \\ 0 & 0 & 0 \\ \vdots & \vdots & \vdots \\ 0 & \kappa_{M-2,M-1}(s) & 0 \\ \kappa_{M-1,M-2}(s) & 0 & \kappa_{M-1,M(s)} \\ 0 & \kappa_{M,M-1}(s) & 0 \end{pmatrix}\begin{pmatrix} A_1(s) \\ A_2(s) \\ \vdots \\ A_m(s) \\ \vdots \\ A_{M-1}(s) \\ A_M(s) \end{pmatrix} \quad (1\text{-}1)$$

where $\kappa(s)$ is the coefficient of coupling between the adjacent turns of MCR and is defined as

$$\kappa(s) = \frac{(n_{eff}^2 - n_e^2)}{\beta}\left\{\frac{2\pi^2}{\lambda^2}\iint_{x^2+y^2<r^2} dxdy[F_{0x}(x,y)F_{0x}(x,y-p(s)) + F_{0y}(x,y)F_{0y}(x,y-p(s))]\right.$$
$$\left. + \frac{1}{2n_{eff}^2}\oint_{x^2+y^2=r^2}\frac{d\ell}{r}(xF_{0x}(x,y)+yF_{0y}(x,y))\left(\frac{\partial F_{0x}(x,y-p(s))}{\partial x}+\frac{\partial F_{0y}(x,y-p(s))}{\partial y}\right)\right\} \quad (1\text{-}2)$$

where the transversal mode $F_0(x, y)$ is normalized as

$$\int_{x^2+y^2<\infty} dxdy\left(F_{0x}(x,y)F_{0x}(x,y)+F_{0y}(x,y)F_{0y}(x,y)\right)=1 \quad (1\text{-}3)$$

In E q. (1-3), n_{eff} and n_e are the effective refractive index of the microfiber and the external refractive index, respectively, and the second integral is taken along the circle

doi:10.6342/NTU201700769

at the surface of the microfiber. F_{0x}(x, y) and F_{0y}(x, y) are the x-direction and y-direction components of the transversal modes and $p(s)$ is the local pitch of the coil. Note that, for the microfiber coil resonators, the output of the i th coil is always equal to the input of the (i+1) th coil, there exists the following continuity conditions [43]

$$\begin{pmatrix} A_1(0) \\ A_2(0) \\ A_3(0) \\ A_4(0) \\ \vdots \\ A_{M-2}(0) \\ A_{M-1}(0) \\ A_M(0) \end{pmatrix} = \begin{pmatrix} 0 & 0 & 0 & 0 & \cdots & 0 & 0 & 0 \\ e^{i\beta\ell} & 0 & 0 & 0 & \cdots & 0 & 0 & 0 \\ 0 & e^{i\beta\ell} & 0 & 0 & \cdots & 0 & 0 & 0 \\ 0 & 0 & e^{i\beta\ell} & 0 & \cdots & 0 & 0 & 0 \\ \vdots & \vdots & \vdots & \vdots & \vdots & \vdots & \vdots & \vdots \\ 0 & 0 & 0 & 0 & \cdots & 0 & 0 & 0 \\ 0 & 0 & 0 & 0 & \cdots & e^{i\beta\ell} & 0 & 0 \\ 0 & 0 & 0 & 0 & \cdots & 0 & e^{i\beta\ell} & 0 \end{pmatrix} \begin{pmatrix} A_1(\ell) \\ A_2(\ell) \\ A_3(\ell) \\ A_4(\ell) \\ \vdots \\ A_{M-2}(\ell) \\ A_{M-1}(\ell) \\ A_M(\ell) \end{pmatrix} + \begin{pmatrix} A_1(0) \\ 0 \\ 0 \\ 0 \\ \vdots \\ 0 \\ 0 \\ 0 \end{pmatrix} \quad (1\text{-}4)$$

where β is the propagation constant of the fundamental mode and ℓ is the perimeter of each turn. The input electric field amplitude is given by $A_1(0)$. By solving the equations above, the MCR transmissivity T is given by

$$T = \frac{A_m(\ell)e^{i\beta\ell}}{A_1(0)} \quad (1\text{-}5)$$

By using the equations and boundary conditions stated above, we can derive the transmission properties of an MCR.

For an optical resonance cavity, the resonance condition is satisfied when the round-trip length of the cavity is equal to an integer multiple of the optical wavelength inside the medium. Once the resonance condition is satisfied, a series of Lorentzian-

doi:10.6342/NTU201700769

shaped transmission curves evenly spaced by the free spectral range (FSR) in the frequency domain. The free spectral range is defined as follows

$$FSR = \frac{\lambda^2}{n_{eff} \times L} \tag{1-6}$$

where λ is the optical wavelength; L is the round trip length of the resonator cavity; n_{eff} is the effective refractive index of the mode propagating in the cavity.

The bandwidths (FWHM) of resonance dips characterize the storage time as the photons propagate inside the cavity and the quality factor is defined as the optical wavelength over the FWHM of the resonance dip of the cavity. The larger quality factor, the longer time of the photons propagating inside the cavity and the more energy is stored. The maximum achievable quality factor of an optical resonator is named as the intrinsic quality factor Q_{int}, which is defined as [44]

$$Q_{\text{int}} = \omega \frac{Stored\ energy}{Power\ loss} = \frac{\beta}{\alpha} \tag{1-7}$$

where ω is the radian frequency; α is the power loss per unit length and β is the propagation constant.

When a resonator is coupled to an external field, the quality factor further decreases due to the loss imported by the coupler. Thus the quality factor is called the external quality factor Q_{ext}, which can be defined as

doi:10.6342/NTU201700769

$$Q_{ext} = \frac{\beta L}{(K - K_m)^2}, \quad K = \kappa L \tag{1-8}$$

where K is the average coupling parameter; K_m is the optimal average coupling parameter; κ is the coupling coefficient. As a result, the final measured quality factor Q_{load} is made up of these two components

$$Q_{load}{}^{-1} = Q_{int}{}^{-1} + Q_{ext}{}^{-1} \tag{1-9}$$

When Q_{load} is equal to Q_{int}, the quality factor is maximized and it only depends on the power loss and operating wavelength. Thus, to achieve the maximum quality factor of an optical resonator, the first priority is to minimize the loss and to make the average coupling parameter approaching to the optimal value.

doi:10.6342/NTU201700769

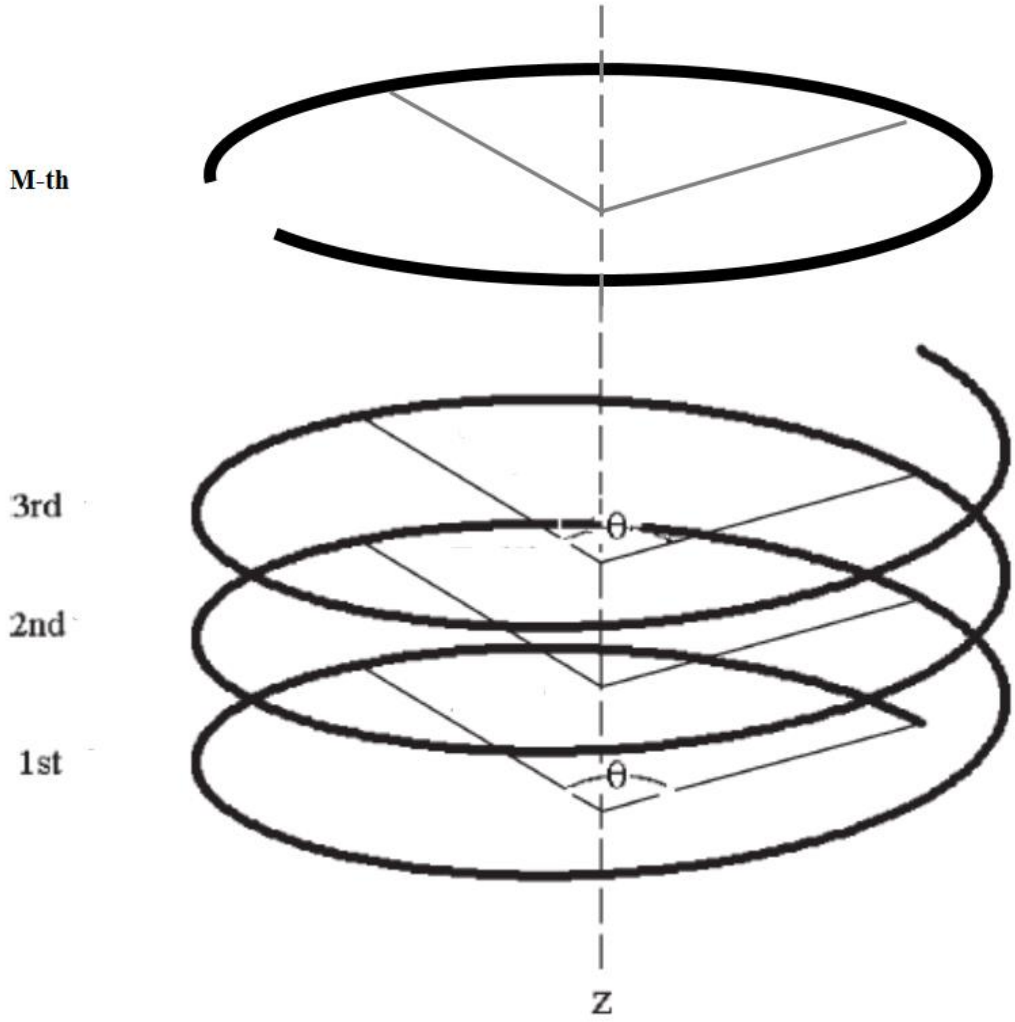

Fig. 1-2 A schematic diagram of MCR.

doi:10.6342/NTU201700769

1.4 Organization of the Thesis

In this thesis, the fabrication of PDMS-packaged microfiber coil resonator with high quality factor is described in details. The refractive index sensitivity of PDMS-packaged MCR is measured and the long-term stability is further improved. Chapter 1 describes the motivation of this thesis and includes literature reviews on up-to-date results reported by other groups worldwide. The theory of MCR is also introduced in Chapter 1. In Chapter 2, the fabrication process of PDMS-packaged MCR is described and the optical characteristics are shown. Chapter 3 shows experiment setup of refractive index sensing and measurement results. The package setup for the rest of microfiber was developed to improve the long-term stability. Chapter 4 is the conclusion of this thesis and future works.

doi:10.6342/NTU201700769

Chapter 2 Fabrication and Optical Characteristics of PDMS-packaged MCRs

2.1 Fabrication of PDMS-packaged MCRs

The fabrication process of PDMS-packaged MCR contains two parts, fabrication of microfiber and coiling process of PDMS-packaged MCR. The microfibers were produced by flame drawing technique with a modified miniature fiber drawing tower since such microfiber could have better surface smoothness and lower propagation loss. Fig. 2-1 shows the experiment setup of a modified miniature fiber drawing tower. The preform used in the experiment was a single-mode optical fiber with core/cladding diameter of 8.2 μm / 125 μm. The hydrogen oxygen flame was applied as heat source. The process of fiber drawing and properties of the microfibers were described in detail in our previous work [45]. By carefully controlling each parameters of drawing tower, a biconical microfiber was fabricated with diameter smoothly varied from the original 125 μm to ~3 μm at the waist section. The waist section could extend over ~150 mm long. The relatively longer waist length could coil more turns on a millimeter-sized silica rod. Before coiled on a silica rod, the microfiber should be cleaned because some particles might be adhered on the surface of microfiber. When the light propagates in

doi:10.6342/NTU201700769

the microfiber, these particles become scattering points and increase propagation loss. Ethanol was used to clean these particles on the surface of microfiber.

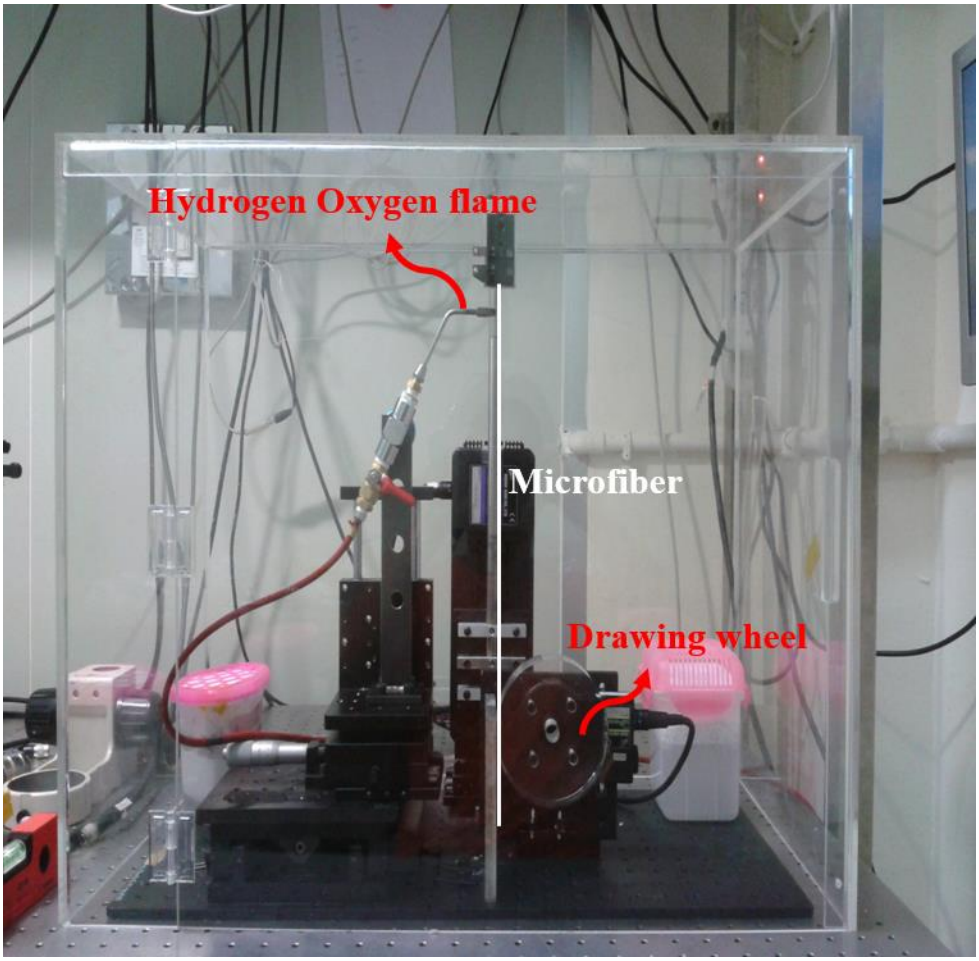

Fig. 2–1 Photograph of modified miniature fiber drawing tower.

doi:10.6342/NTU201700769

Fig. 2-2 (a) and (b) show the schematic diagram for the fabrication of MCR and the photograph of the fabrication system respectively. A fiber holder, a coiling disc, and a socket set to clamp the rod were connected with a rotation stage. The whole structures mentioned above were designed to achieve good concentricity and stability. The assembly steps of each components and calibration method were described in detail in our prior work [45].

A Teflon bar (n ~1.3) fixed on a motorized stage was used to control the gaps between microfibers. A V-shaped groove was carved on the Teflon bar. The microfiber was caught in the V-shaped groove by tension. Fig. 2-3 shows the top view photograph of the V-shaped groove. A manual z-axis stage was mounted beneath the motorized stage to make the Teflon bar and silica rod at the same height. As shown in Fig. 2-4, a bevel was placed at each corner of the Teflon bar to prevent microfiber from damage.

During the coiling process, the gap between microfibers was observed by a monocular microscope and a CCD. To have enough space to coil microfiber and enough resolution to identify gap, an extra long working distance objective was chosen. With the help of these devices, the coiling process could be observed *in situ*.

For a bare MCR, the structural stability is maintained by the Van der Waals force between microfibers and PDMS-coated silica rod. The weak stability makes it hard to take MCR from coiling disk without changing structure. Fig. 2-5 shows the result after

doi:10.6342/NTU201700769

a 0.1 μL ethanol dropped on a bare MCR. The MCR turns were misplaced, which would severely affect the performance of MCR. Therefore, proper packaging MCR is essential before MCR applications.

A silica rod with diameter 1.8 mm was used as a cylindrical brace and coated with PDMS to avoid mode leakage between microfiber coil and silica rod. The lower part of microfiber was placed in the V-shape groove on the Teflon bar, and then the upper part was fixed on the fiber holder. Before coiling process started, the PDMS-coated silica rod was spread with 0.1 μL hexane-diluted PDMS by pipette. The uncured hexane-diluted PDMS was used as package material. A PDMS pre-polymer to curing agent ratio of 10:1 was used. The dilution ratio of PDMS to hexane by weight was 2:1. The purpose of diluting PDMS with hexane is to reduce the viscosity of PDMS [46]. During coiling process, the microfiber coil should be turned back when the faults were detected. If PDMS was spread without dilution, the microfiber would stick on rod and the coil could not be turned around. Hexane-diluted PDMS has lower viscosity so the microfiber coil could be turned around easily.

During the coiling process, the microfiber coil immersed in the uncured hexane-diluted PDMS. Then MCR in hexane-diluted PDMS was cured by infrared heat lamp for 2 hours. Fig. 2-6 shows the photograph of a PDMS-packaged MCR by coiling 3 μm diameter microfiber with 3 turns.

doi:10.6342/NTU201700769

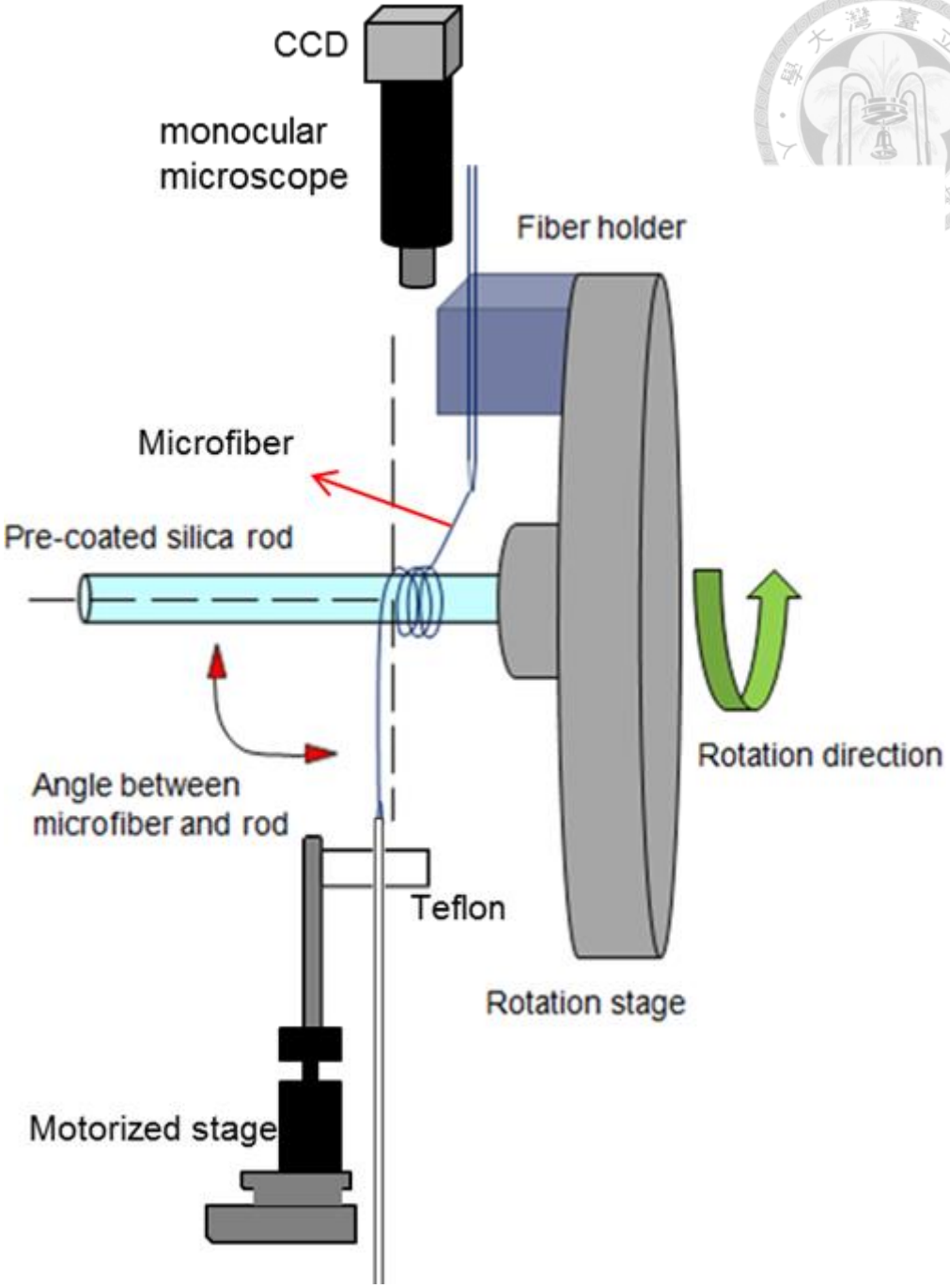

Fig. 2-2 (a) Schematic setup for fabrication of MCRs.

doi:10.6342/NTU201700769

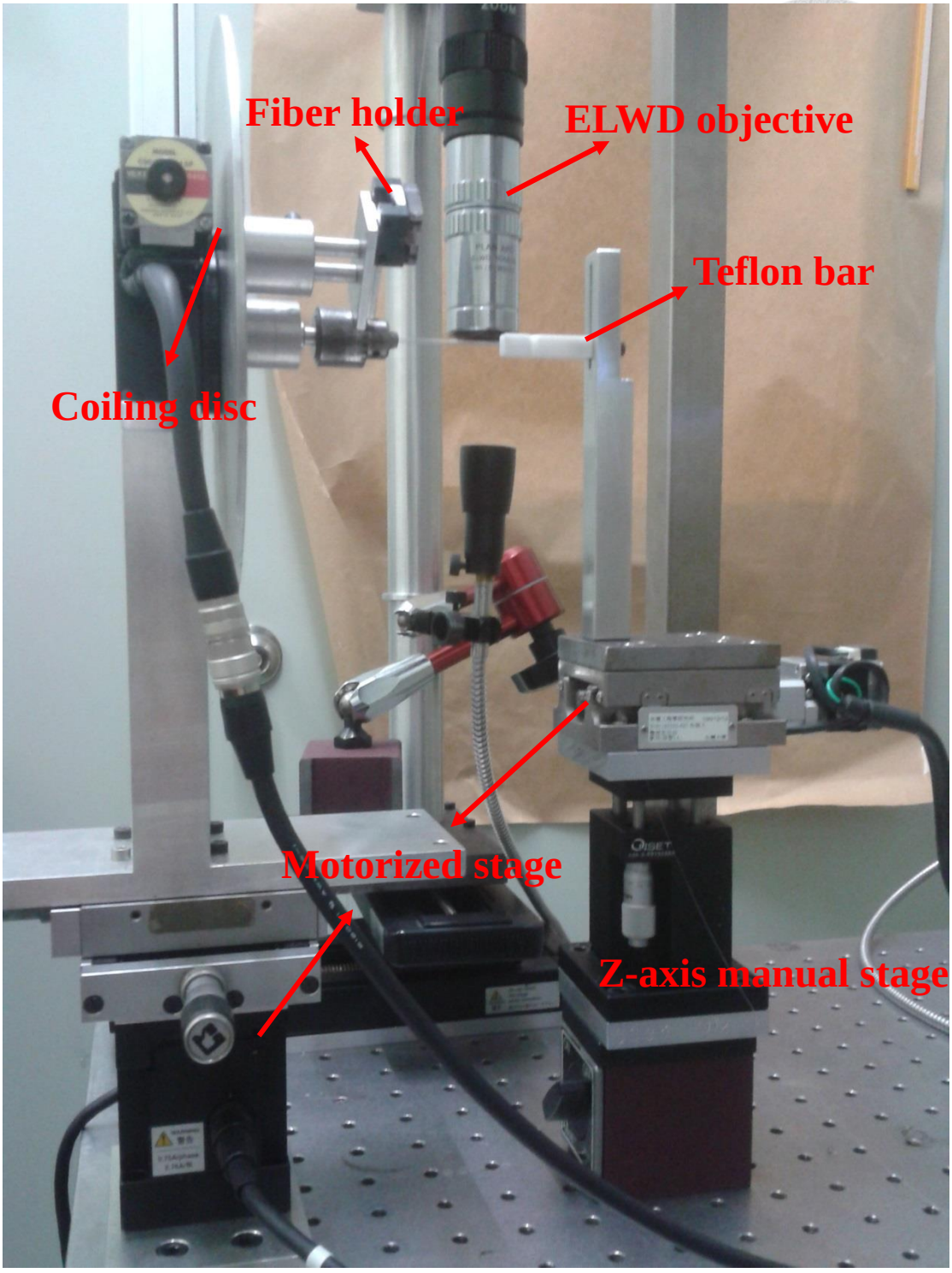

Fig. 2-2 (b) Photograph of the fabrication system.

doi:10.6342/NTU201700769

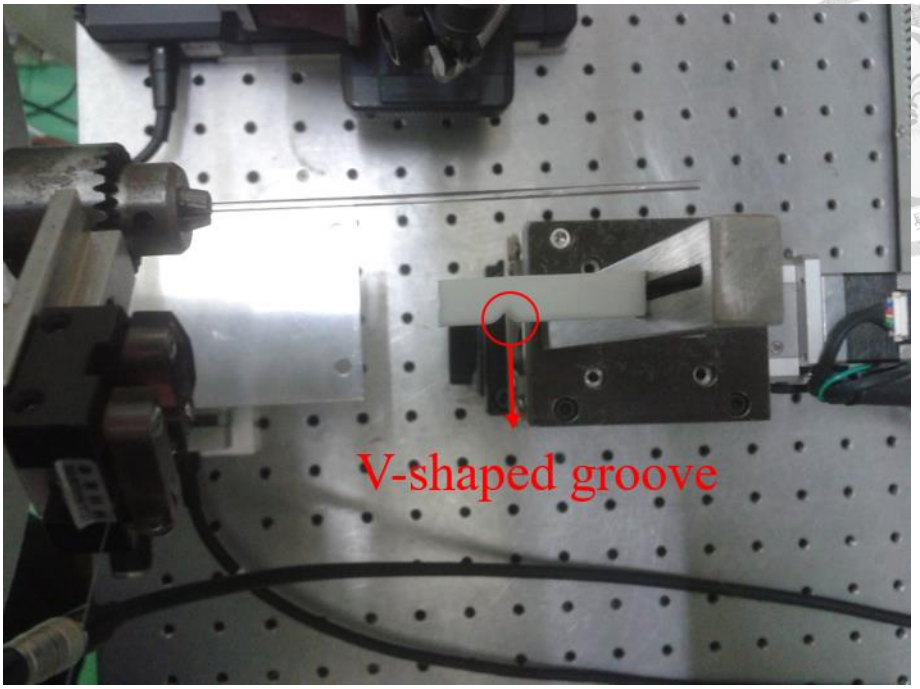

Fig. 2-3 Top view of V-shaped groove carved on the Teflon bar.

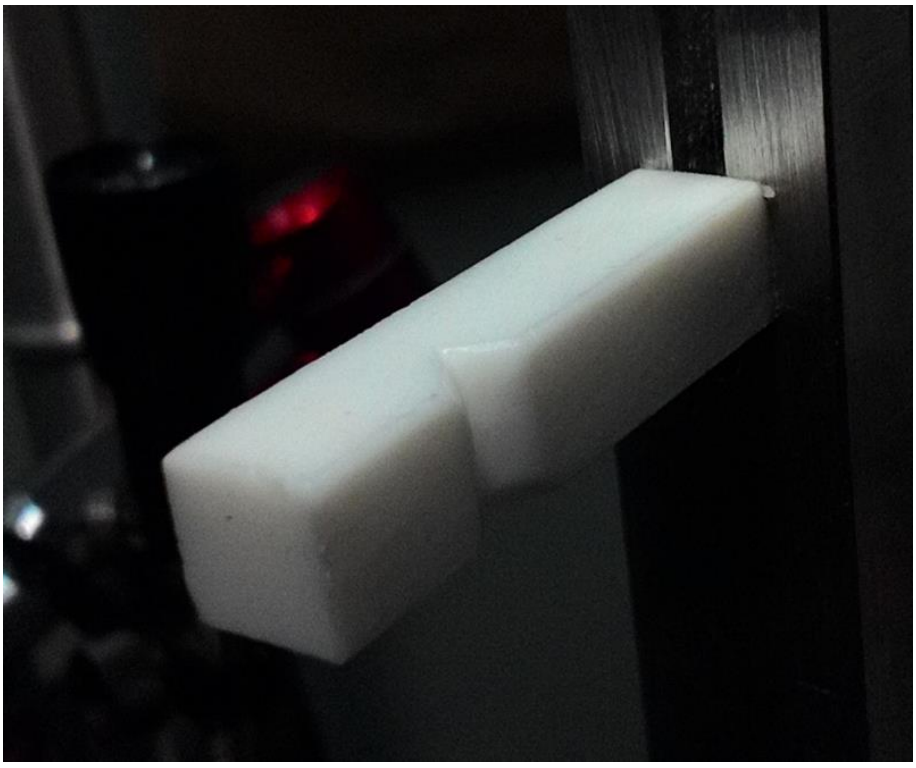

Fig. 2-4 Photograph of bevel of Teflon bar.

doi:10.6342/NTU201700769

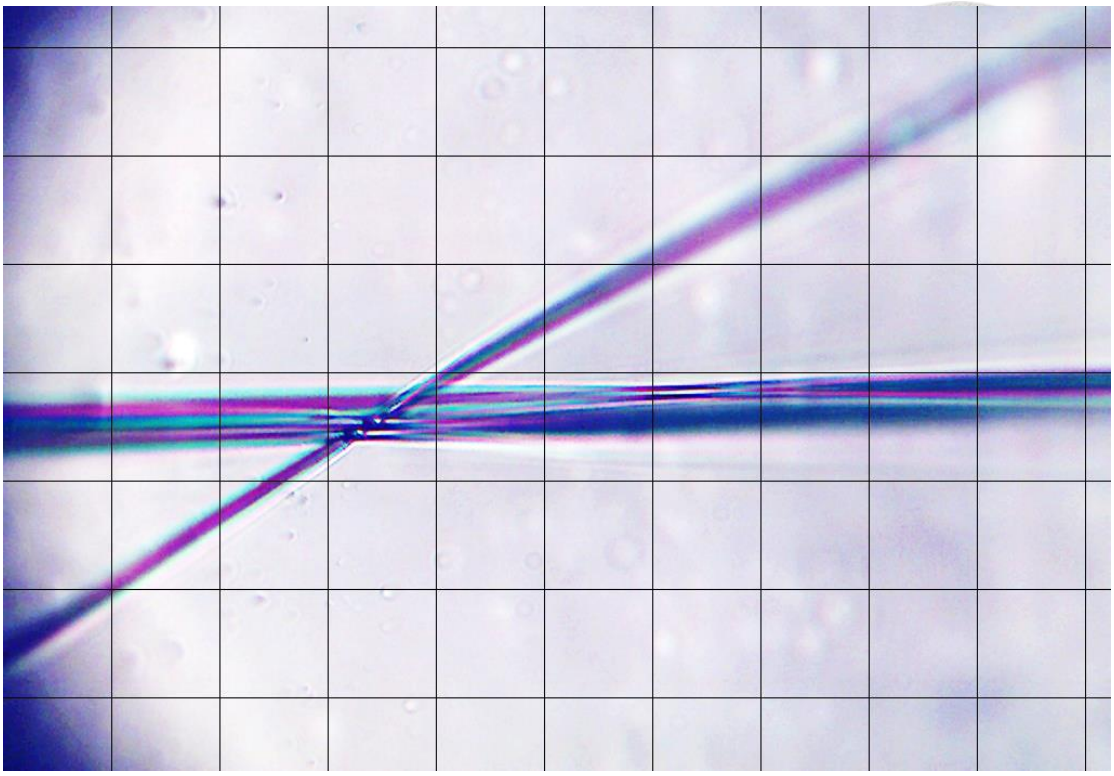

Fig. 2-5 Photograph of a bare MCR after ethanol was dropped on it.

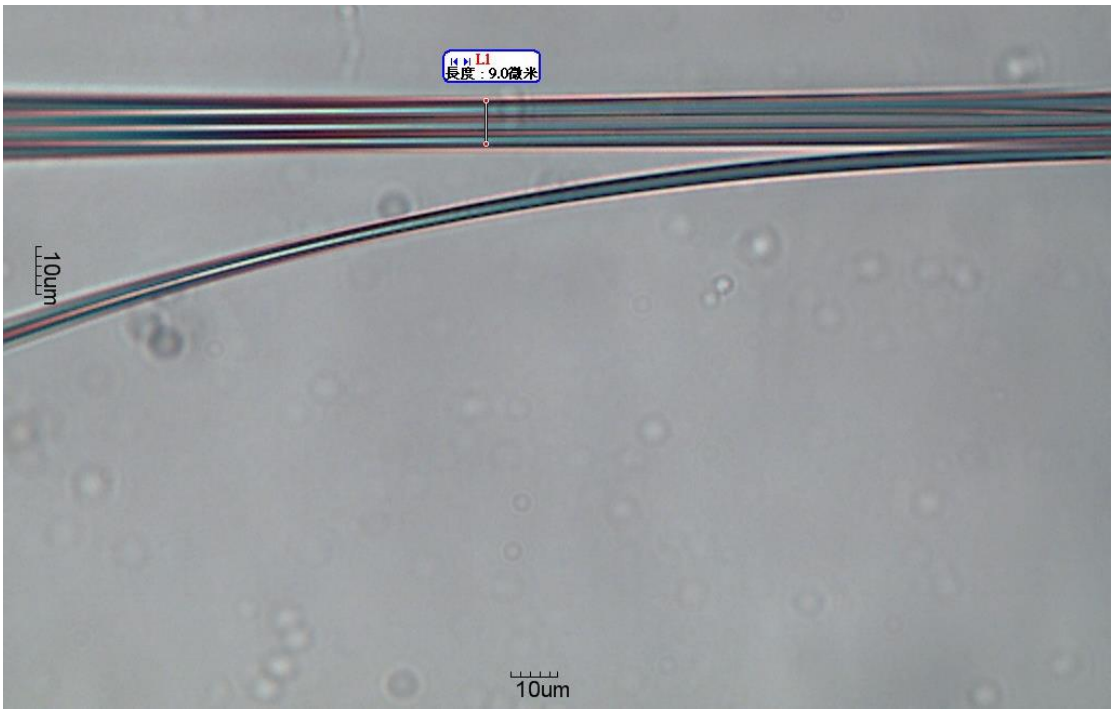

Fig. 2-6 Photograph of PDMS-packaged MCR with 3 turns.

doi:10.6342/NTU201700769

2.2 Optical Characteristics of PDMS-packaged MCRs

To measure the transmission spectrum of a PDMS-packaged MCR, a tunable continuous wave laser source (Phoenix 1400, LUNA) controlled by a desktop computer was used as light source. An isolator was used to prevent the laser source from damage because of back-reflection. The transmission spectrum was detected by the built-in photodetector in the tunable laser source. Fig. 2-7 shows the transmission spectra of the MCR before and after curing the hexane-diluted PDMS. The difference between two spectra might result from the hexane-diluted PDMS. During the curing process, hexane-diluted PDMS slowly flowed due to gravity, which might change the resonant condition.

The measured transmission spectrum of PDMS-packaged MCR is shown in Fig. 2-8 (a). The free spectral range was 0.295 nm, and the extinction ratio was ~10 dB. Lorentzian curve fitting was applied to determine the bandwidth of dip. As seen in Fig. 2-8 (b), the bandwidth of the resonant dip at 1551.186 nm was 3.1 pm and the quality factor ($\lambda / \Delta \lambda$) was ~510,000. To verify the stability of PDMS-packaged MCRs, the power evolution of bare and PDMS-packaged MCRs were recorded over 5 days at 1550 nm. As shown in Fig 2-9, the transmission power of a bare MCR decreased at the rate of ~0.25 dB/hr, while a PDMS-packaged MCR almost remained at the same level. The result showed that packaging MCR with PDMS could prevent MCR from degradation.

doi:10.6342/NTU201700769

Fig. 2-10 shows both the simulated and the experimental results. The simulation was computed by Matlab. The parameters used in the simulation were the same as those in the experiment, namely rod diameter 1.8 mm, microfiber diameter 3 μm and PDMS refractive index 1.402. Compared with the simulated result, some resonance dips of experimental spectrum are suppressed and have blue shift. This might be attributed to the flow of hexane-diluted PDMS during curing process.

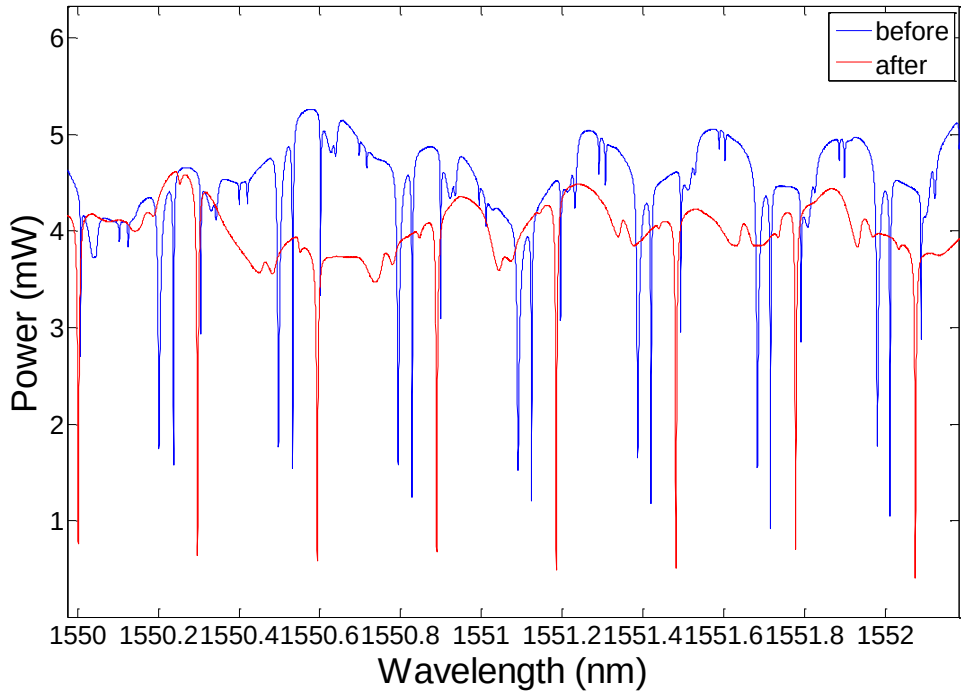

Fig. 2-7 Transmission spectra of MCR before (blue line) and after (red line) curing.

doi:10.6342/NTU201700769

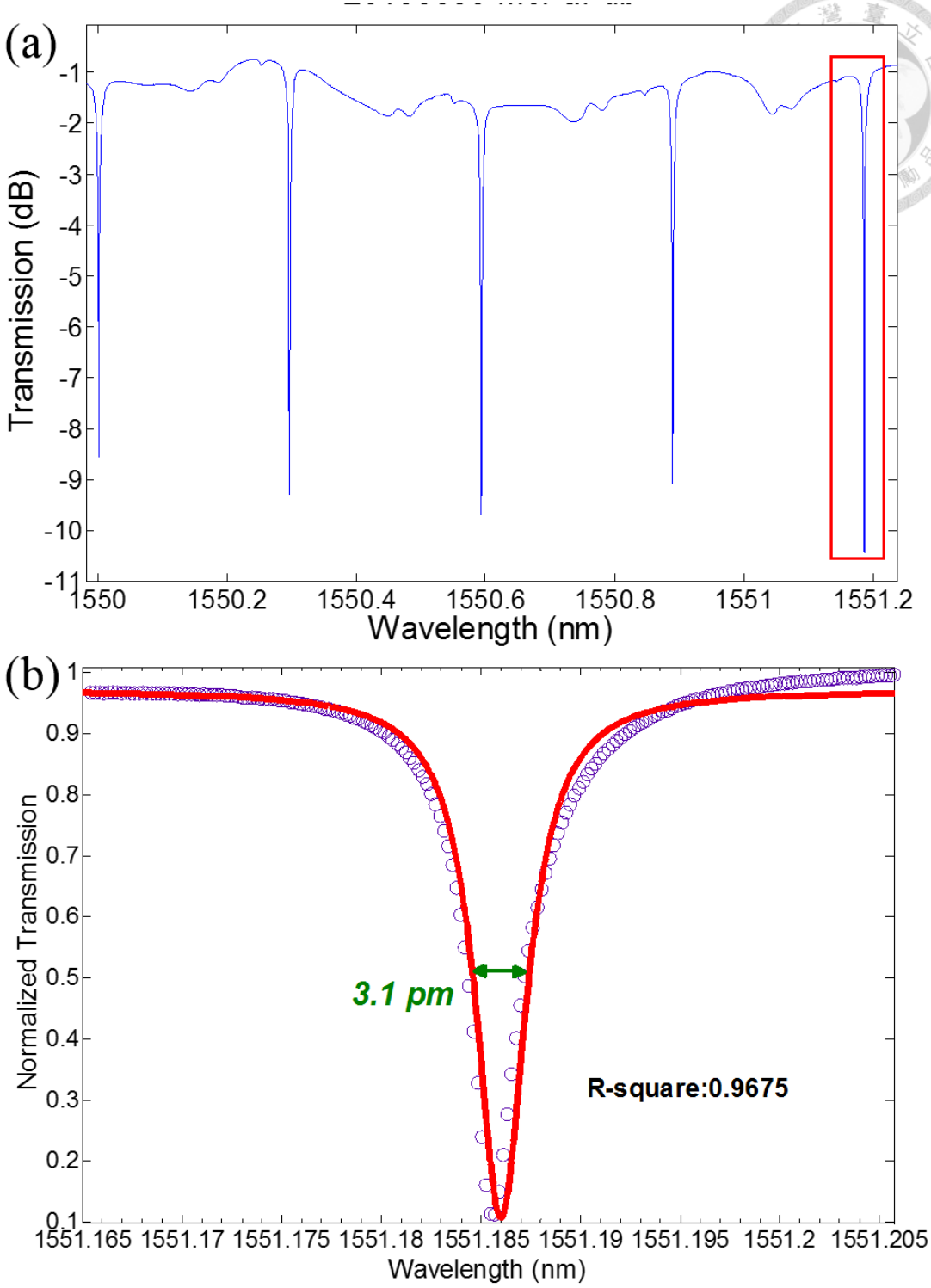

Fig. 2-8 (a) Transmission spectrum of PDMS-packaged MCR and (b) one resonant dip and its Lorentz curve fitting.

doi:10.6342/NTU201700769

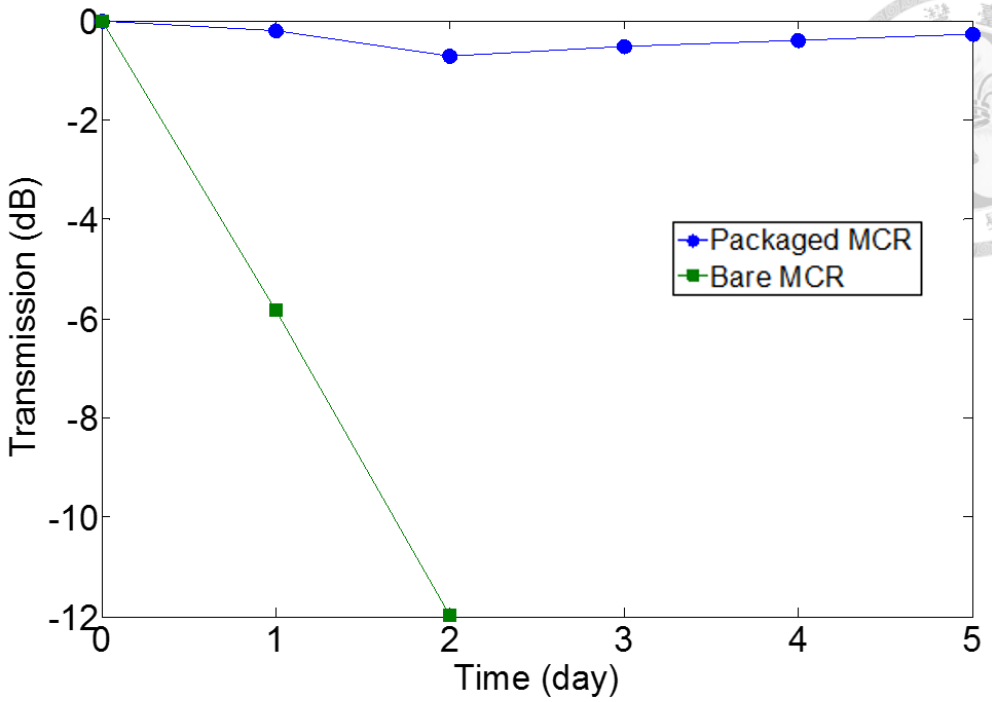

Fig. 2-9 Power evolutions of a bare (green) and a PDMS-packaged (blue) MCRs over 5 days measured in 1550 nm wavelength.

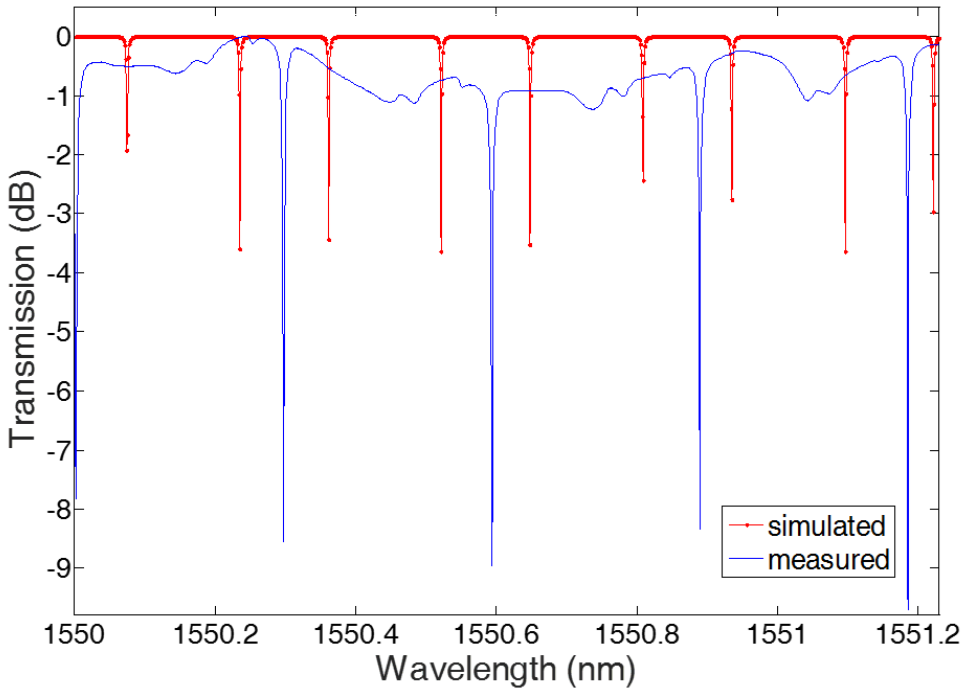

Fig. 2-10 Transmission spectra of simulated (red line) and measured (blue line) PDMS-packaged MCR.

doi:10.6342/NTU201700769

Chapter 3 Refractive Index Sensing and Long-term Stability Improvement

3.1 Experimental Setup of Refractive Index Sensing

MCRs with high quality factor have sharp dips at resonant wavelengths. Such sharp dips implies the small amount of resonant wavelength shifts could be distinguished. So high-Q MCRs could serve as refractive index sensors with low detection limit.

To measure the sensitivity of PDMS-packaged MCR to refractive index (RI) variation, a PDMS-packaged MCR was taken from coiling system gently and then fixed on a clip shown in Fig. 3-1. To make the sensing structure more stable, a four-layer polymethylmethacrylate (PMMA) structure was used to support the PDMS-packaged MCR for analyte detection. The dimensions of four PMMA plates are shown in Fig. 3-2. The PMMA structure was fabricated by bonding four 2 mm thickness PMMA plates in sequence. Fig. 3-3 (a) and (b) show the photographs of PDMS-packaged MCR in the PMMA structure. The red part of PMMA structure in Fig. 3-3 (b) was coated with PDMS to avoid light leakage when microfibers touched this region.

For the experiment of RI sensing, the glucose solutions with different

doi:10.6342/NTU201700769

concentrations were used as the surroundings in order to have RI ranged from 1.33 to 1.34. Table 3-1 shows the concentrations expressed in mass fraction and the corresponding RIs, which were measured by using a portable refractometer (RA-130, Kyoto Electronics) and data were taken five times for each concentration and then averaged. The averaged results show small standard deviations.

Next, the glucose solutions were slowly dropped into RI sensing region as shown in Fig. 3-3 (b) by using pipet until solutions were filled in the sensing region. Then the packaged MCR was directly immersed in the glucose solutions. Fig. 3-4 shows the photograph of a PDMS-packaged MCR during RI sensing. The transmission spectra of PDMS-packaged MCR in each glucose solutions were measured three times. These transmission spectra were measured by using the same PDMS-packaged MCR. After each measurement of the solution of a given RI, the solution was pumped out and the PDMS-packaged MCR was flushed gently with deionized water.

doi:10.6342/NTU201700769

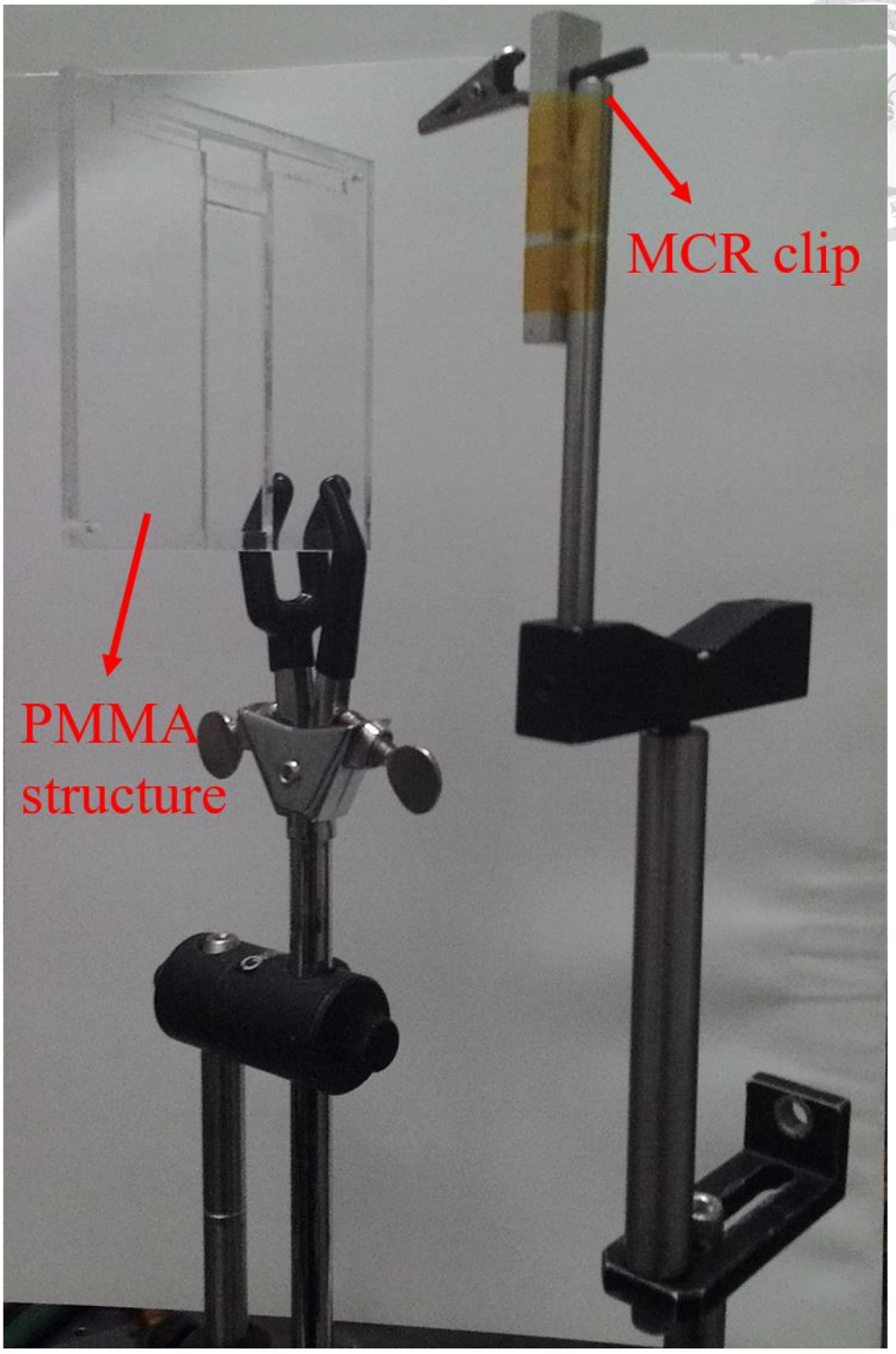

Fig. 3-1 Photograph of 4-layer PMMA structure and MCR clip.

doi:10.6342/NTU201700769

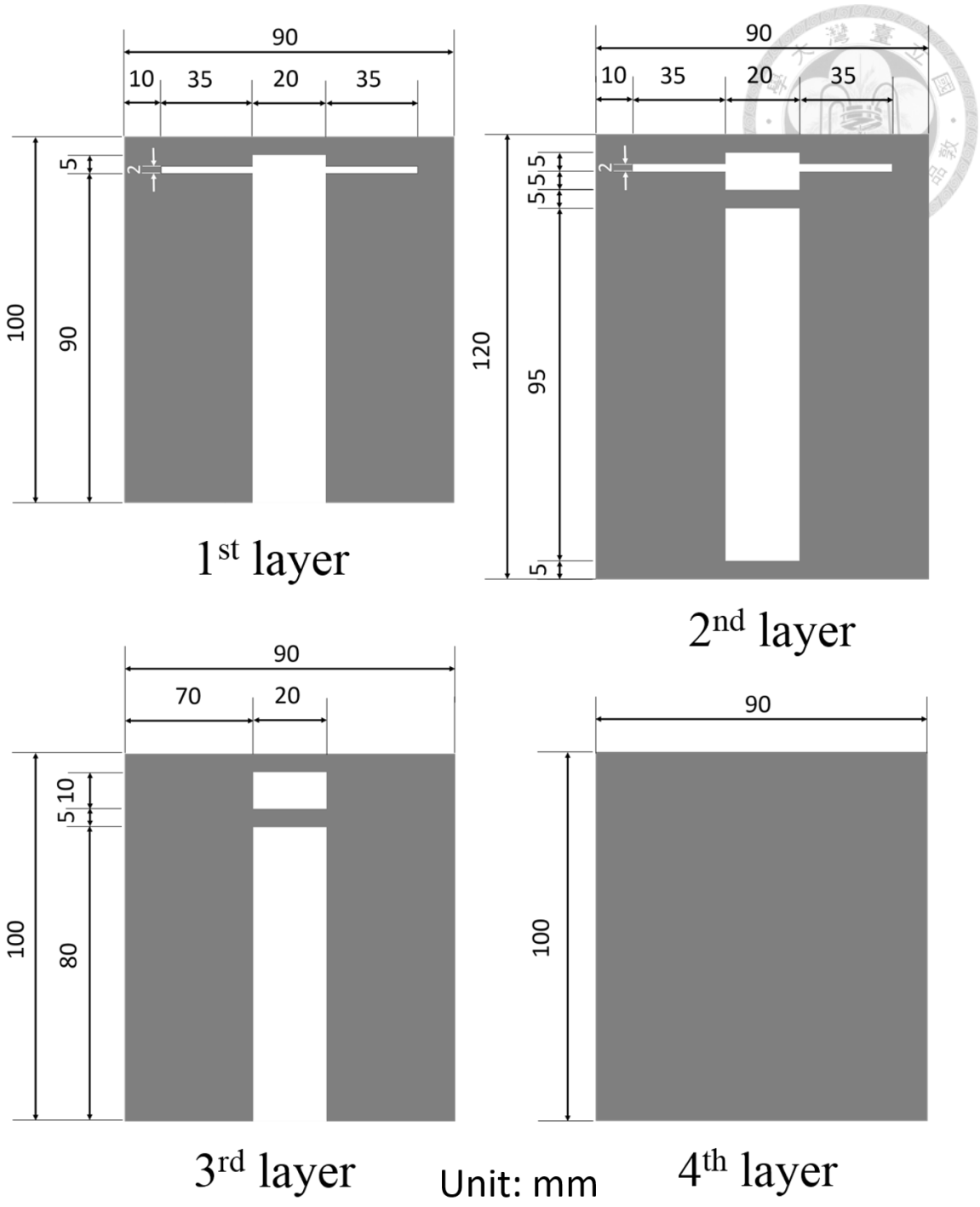

Fig. 3-2 Dimensions of four PMMA plates for PMMA structure.

doi:10.6342/NTU201700769

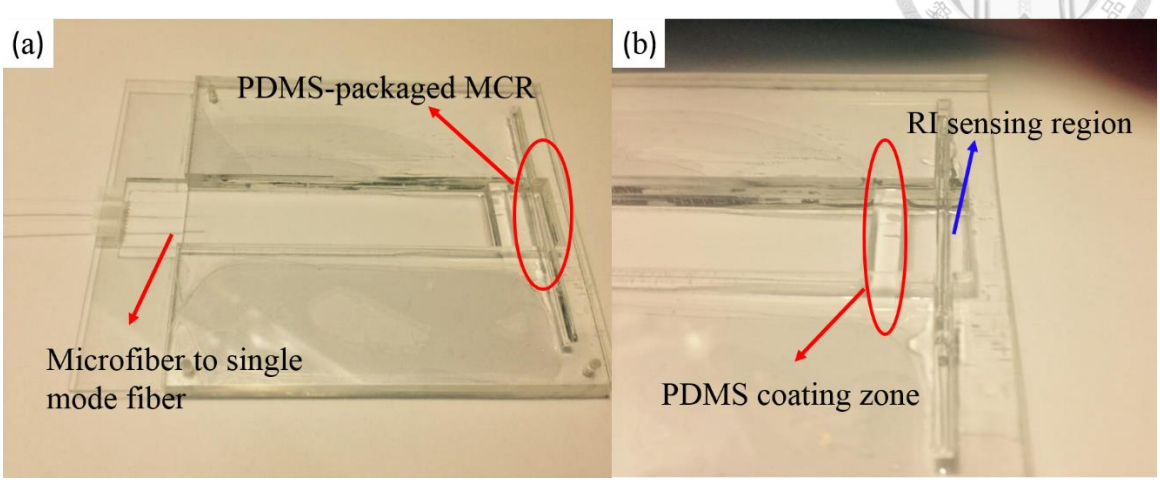

Fig. 3-3 (a) Photograph of PDMS-packaged MCR in PMMA structure. (b) Close-up photo of PDMS coating zone and RI sensing region.

Concentration (w/w %)	Refractive Index (avg.)	Standard Deviation
0	1.3332	0.000109
2	1.3355	0.000040
4	1.3382	0.000074
6	1.3412	0.000048
8	1.3437	0.000040
10	1.3468	0.000080

Table 3-1 Refractive indices for the glucose solutions with different concentrations.

doi:10.6342/NTU201700769

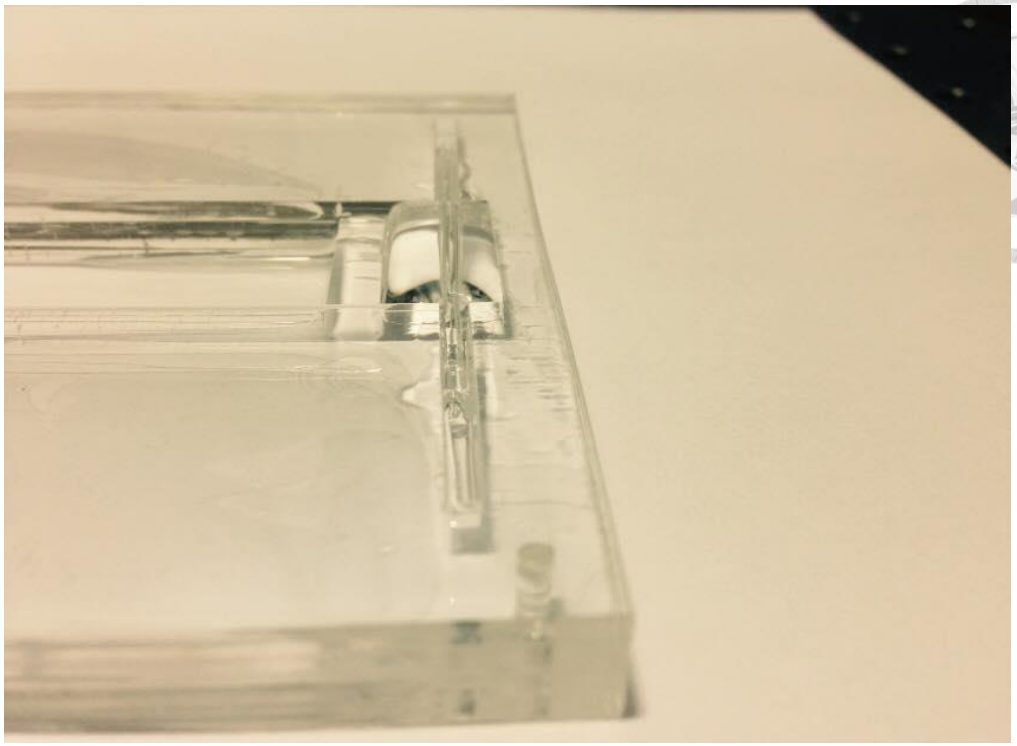

Fig. 3-4 Photograph of a PDMS-packaged MCR during RI sensing.

doi:10.6342/NTU201700769

3.2 Measurement Results and Discussion

The transmission spectrum of PDMS-packaged MCR before RI sensing is shown in Fig. 3-5. The averages and standard deviations of wavelength shifts for different glucose solutions are listed in Table 3-2. Fig. 3-6, 3-7 and 3-8 show the measured transmission spectra of the PDMS-packaged MCR in each glucose solutions and the shifts of the resonant dips in the transmission spectra which were measured three times for each. These spectra correspond to the wavelength shift in Table 3-2. The resonant dips shifted to longer wavelengths as the glucose concentration increased. The spectrum of PDMS-package MCR exposed in air is not shown in the figure for the clear display of the dips in the range of 1546.92-1547.01 nm. To estimate the sensitivity of the PDMS-packaged MCR, the average wavelength shift and standard deviations of each RI in Table 3-2 were fit and plotted and the result is shown in Fig. 3-9. The slope of the linear fit is 5.592 nm/RIU and it corresponds to the sensitivity of PDMS-packaged MCR. In a previous study by Fei Xu *et. al.*, a Teflon-coated MCR has been applied as a refractometric sensor with quality factor ~ 10^4. The measured refractive index ranged from 1.345 to 1.349 and sensitivity was about 40 nm/RIU [22]. The main reason of low sensitivity is due to the high quality factor of packaged MCR. A resonator with high quality factor has better optical confinement; however, high sensitivity requires more

doi:10.6342/NTU201700769

evanescent field to interact with the analytes [47], which implies less optical confinement. Therefore, there is a trade-off between quality factor and sensitivity. The other reason is that the PDMS packaging limits the interaction between evanescent field and analytes. The PDMS packaging layer reduces the overlap between evanescent field outside microfiber and analytes, which equivalently decreases the effective index change of the propagating modes in MCR. The microfiber-based resonator with high quality factor is thus better used for the application which need detection limit due to its narrower bandwidth. The detection limit 1/*P* is defined as [47]:

$$1/P \equiv \mathrm{FWHM}/S$$

where FWHM is the bandwidth of MCR and S is the sensitivity. The larger P is, the lower the detection limit is. For our PDMS-packaged MCR with quality factor ~500,000, the detection limit is about 7×10^{-4} RIU. Detection limit reported in Ref. 22 was about $4\text{x}10^{-3}$ RIU. Compared with Ref. 22, our PDMS-packaged MCR has a lower detection limit due to higher quality factor.

The recycle ability of PDMS-packaged MCR in RI sensing is remained to be solved. During RI sensing, microfibers extended from PDMS-packaged MCR were also immersed in glucose solutions and some particles might attach on microfibers. As shown in Fig. 3-10, these particles were difficult to be totally removed even with repeated clean. These particles were very likely glucose residue. Fig. 3-11 shows the

doi:10.6342/NTU201700769

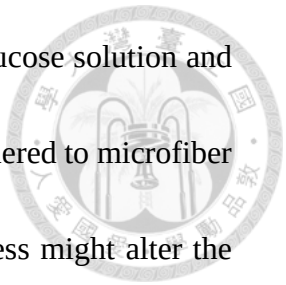

photograph of two microfibers after they were immersed in 30% glucose solution and deionized water separately. It is obvious that more particles were adhered to microfiber after immersed in glucose solution. Also, microfiber drawing process might alter the silica surface by formation of hydroxyl group. Hydroxyl group would enhance the interaction between analyte and silica because of attractive forces, which makes particles adhere to microfiber more likely [48]. The additional scattering loss due to these particles had negative impact on the performance of PDMS-packaged MCR. As shown in Fig. 3-12, the power level decayed after RI sensing. Fig. 3-13 (a) and (b) show that the bandwidth of resonant dip became wide after RI sensing. To achieve the recycle ability, microfibers should also have low refractive index coating. PDMS cured by CO_2 laser has been put into the test of microfiber coating. However, there were some problems in PDMS coating process. The PDMS coating should be cured rapidly. Otherwise, the coating would shrink into ball shape owing to the surface tension of PDMS. Besides, it is difficult to stretch the microfiber of a MCR to be straight. The PDMS coating would not be uniform on loose microfibers.

doi:10.6342/NTU201700769

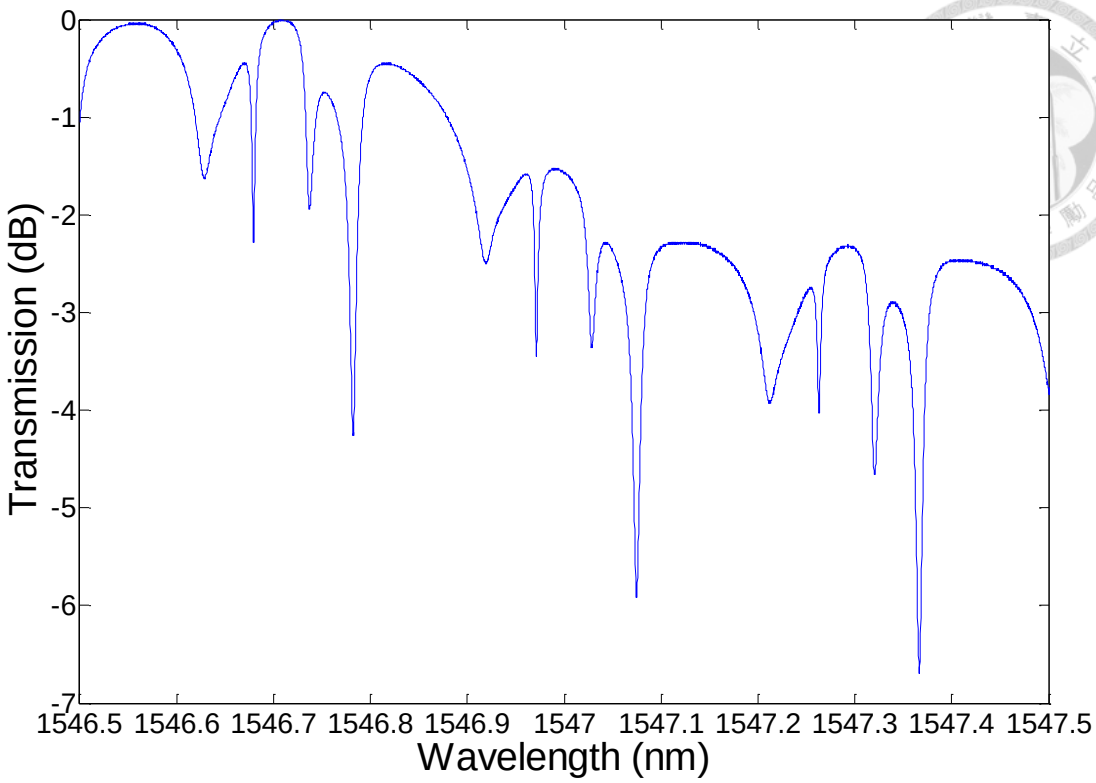

Fig. 3-5 Transmission spectrum of PDMS-packaged MCR before RI sensing.

Concentration (w/w %)	Wavelength shift (nm)				
	1	2	3	Average	Standard deviation
2	0.0034	0.0029	0.0024	0.0029	0.00050
4	0.0243	0.0221	0.0211	0.0225	0.00163
6	0.0375	0.0303	0.0341	0.0340	0.00360
8	0.0467	0.0375	0.0436	0.0426	0.00468
10	0.0689	0.0551	0.0534	0.0591	0.00850

Table 3-2 Values, averages and standard deviations of wavelength shift at different glucose solutions.

doi:10.6342/NTU201700769

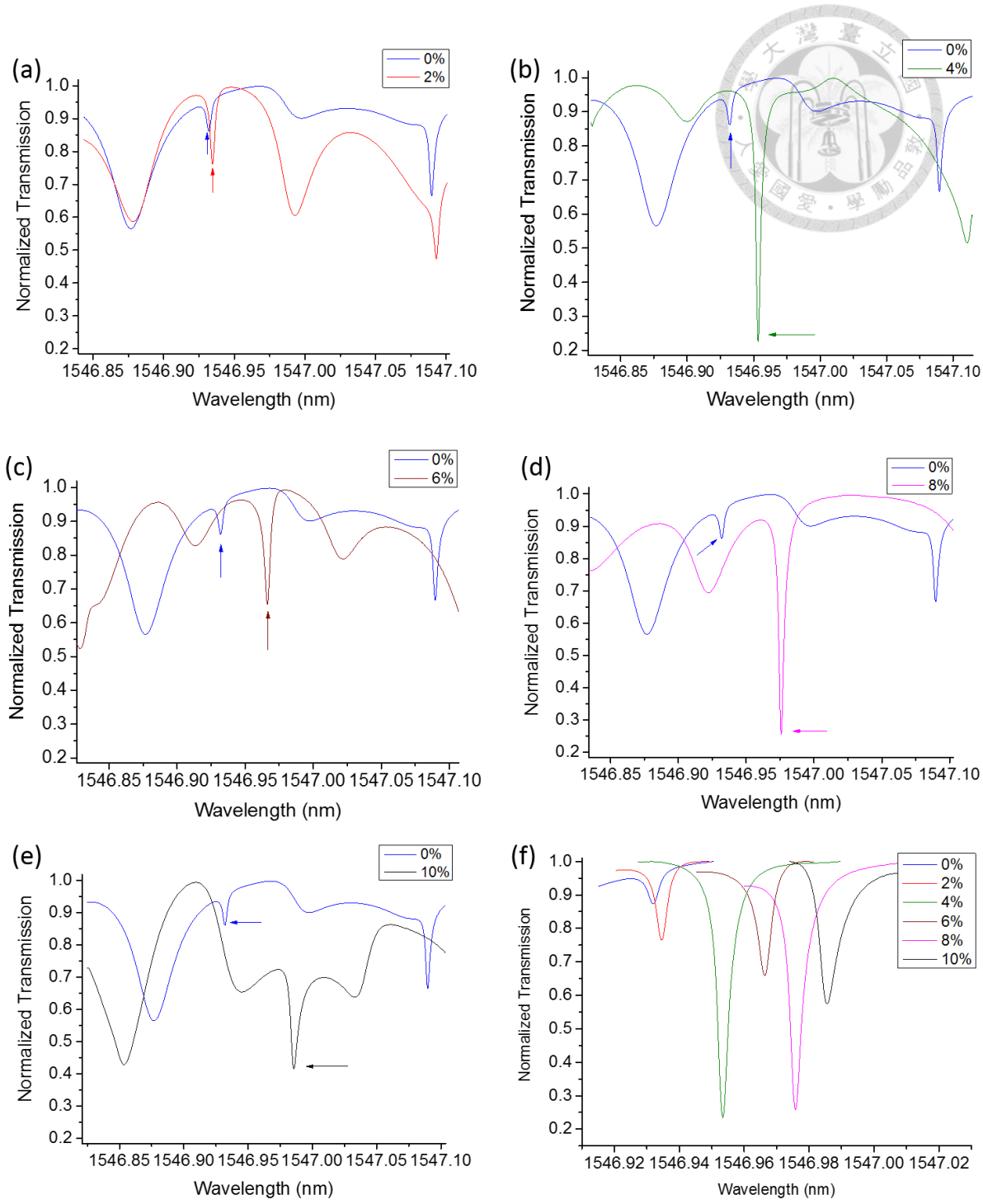

Fig. 3-6 (a)-(e) Measured transmission spectra of PDMS-packaged MCR in each glucose solutions of first measurement. (f) The shifts of the resonant dip in the transmission spectra.

doi:10.6342/NTU201700769

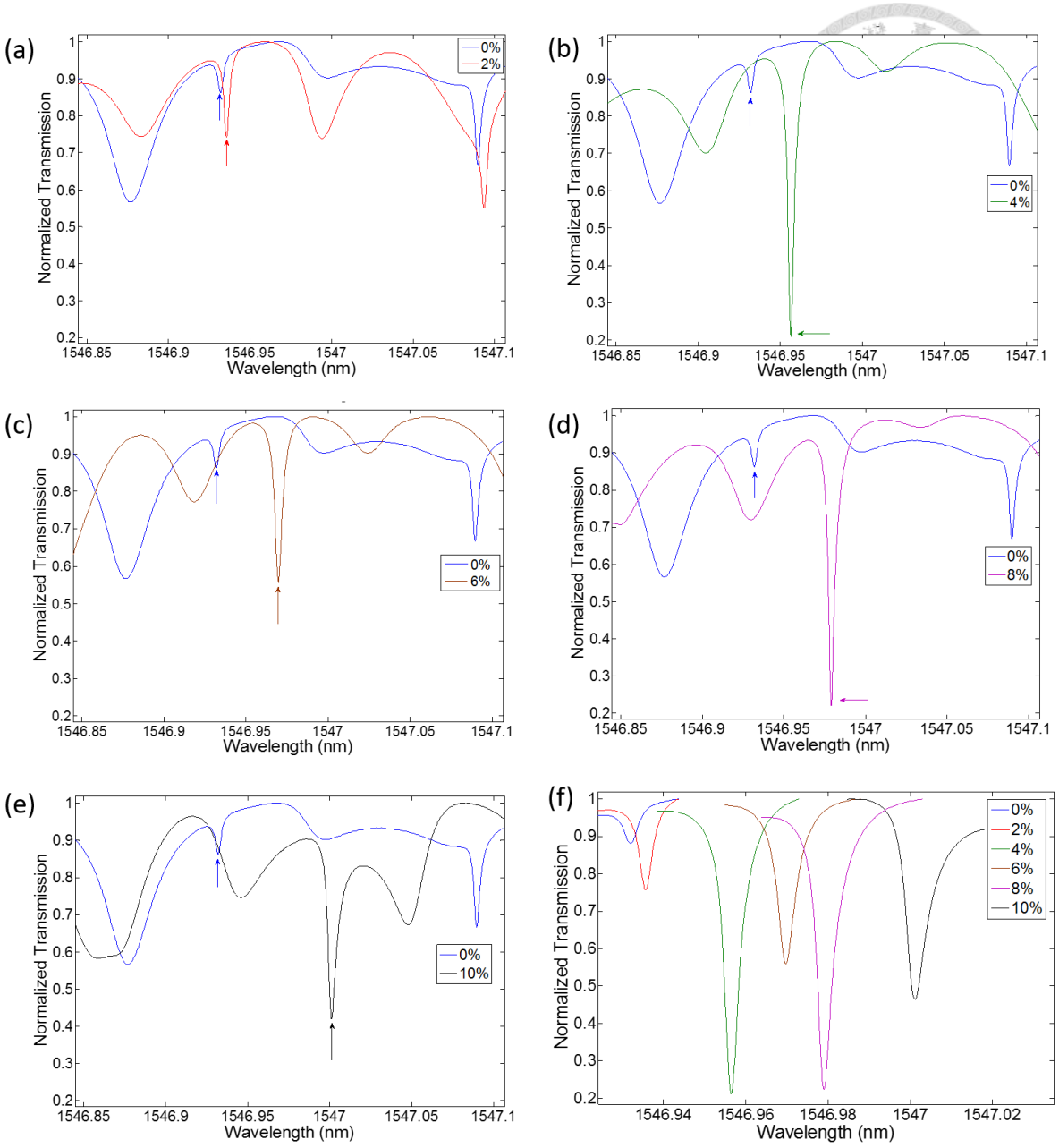

Fig. 3-7 (a)-(e) Measured transmission spectra of PDMS-packaged MCR in each glucose solutions of second measurement. (f) The shifts of the resonant dip in the transmission spectra.

doi:10.6342/NTU201700769

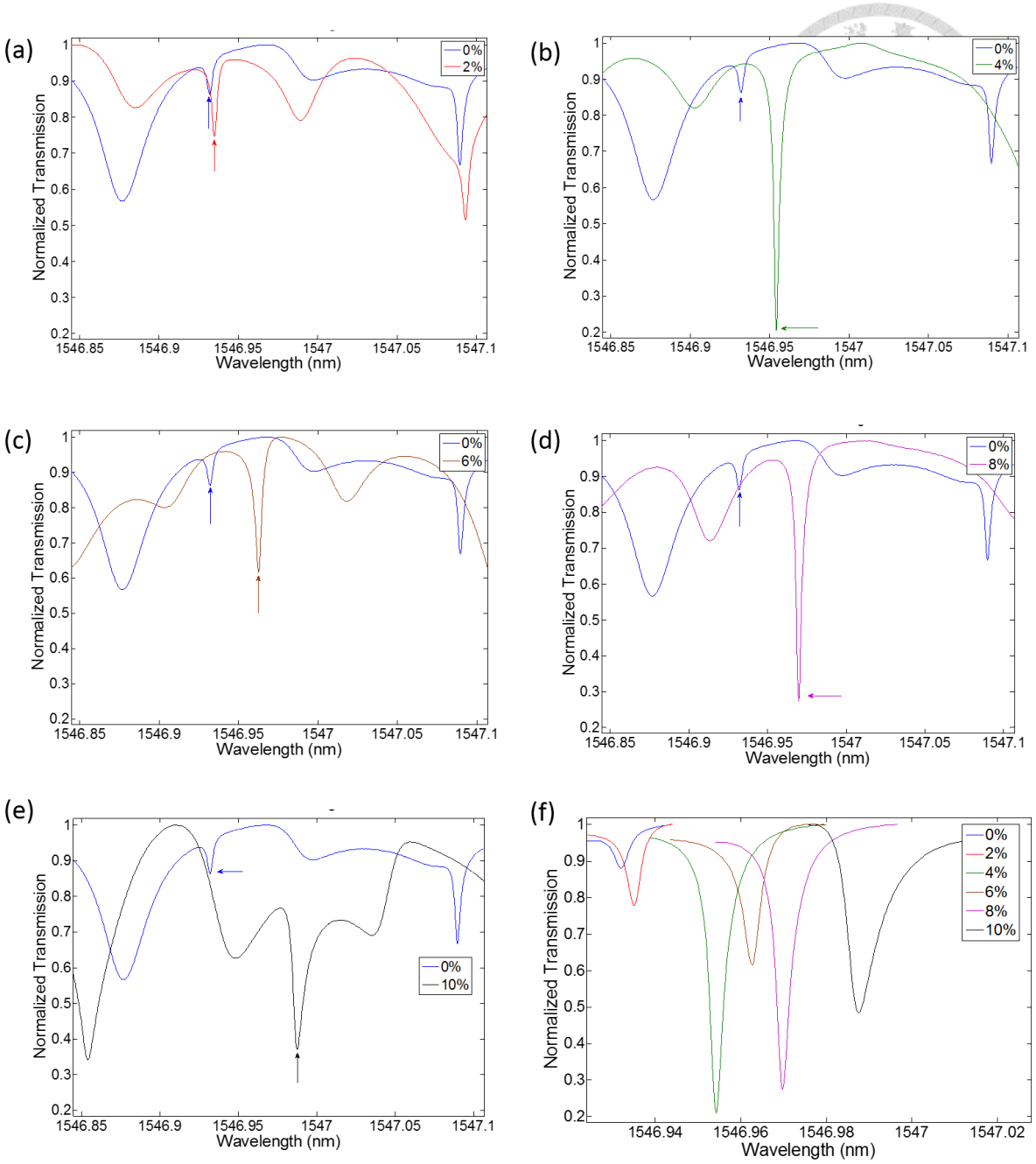

Fig. 3-8 (a)-(e) Measured transmission spectra of PDMS-packaged MCR in each glucose solutions of third measurement. (f) The shifts of the resonant dip in the transmission spectra.

doi:10.6342/NTU201700769

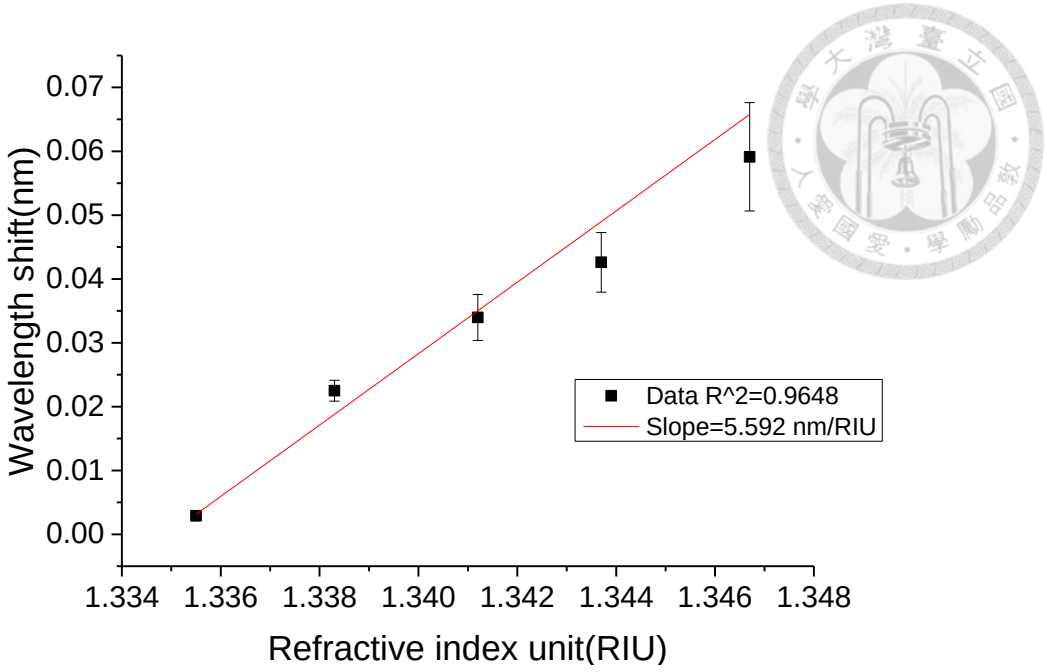

Fig. 3-9 Dependence of the measured wavelength shifts on the refractive index of glucose solutions and its linear fit to the data.

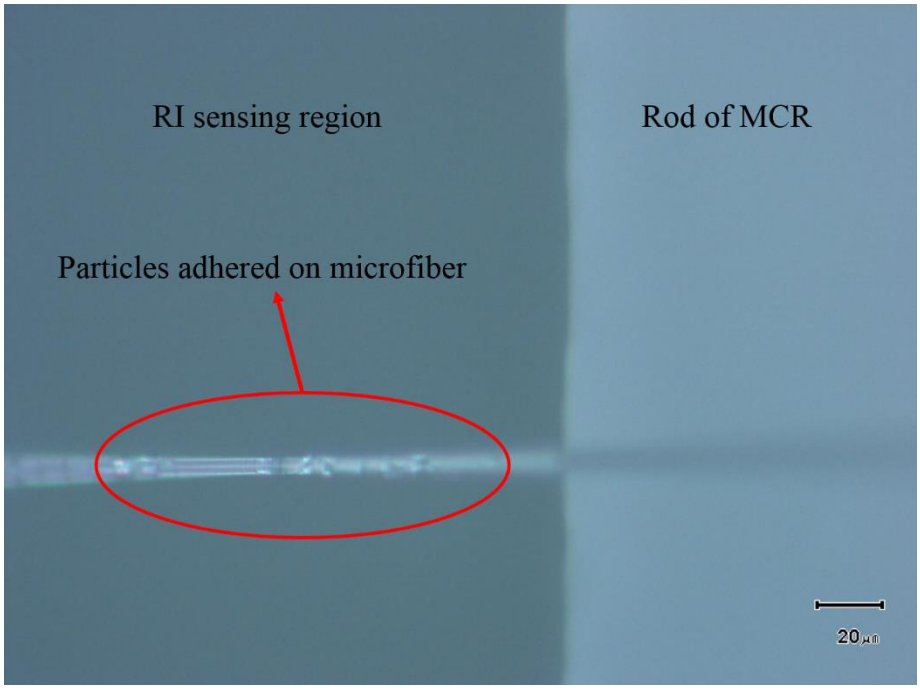

Fig. 3-10 Microscopic image of microfiber in the RI sensing region after RI sensing.

doi:10.6342/NTU201700769

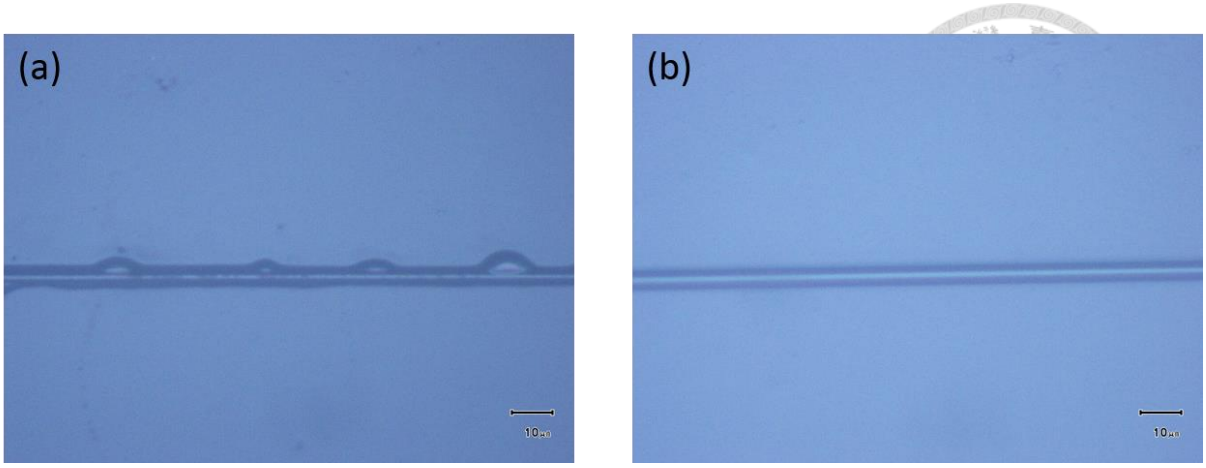

Fig. 3-11 Photograph of microfibers after they were immersed in (a) 30% glucose solution and (b) deionized water.

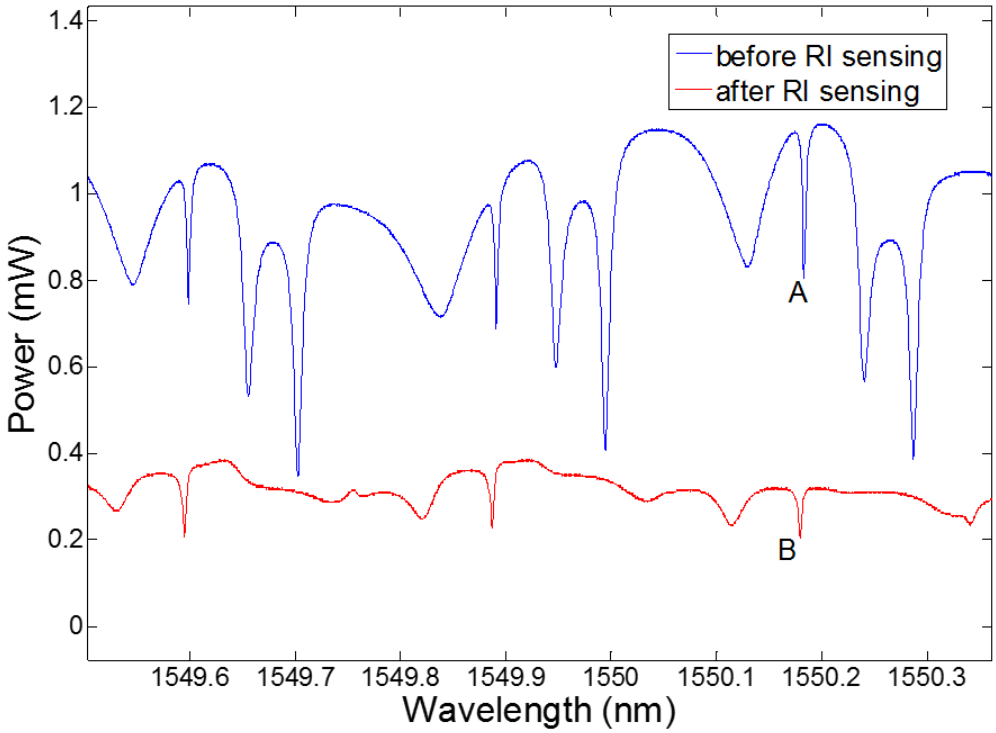

Fig. 3-12 Transmission spectra of PDMS-packaged MCR before and after RI sensing.

doi:10.6342/NTU201700769

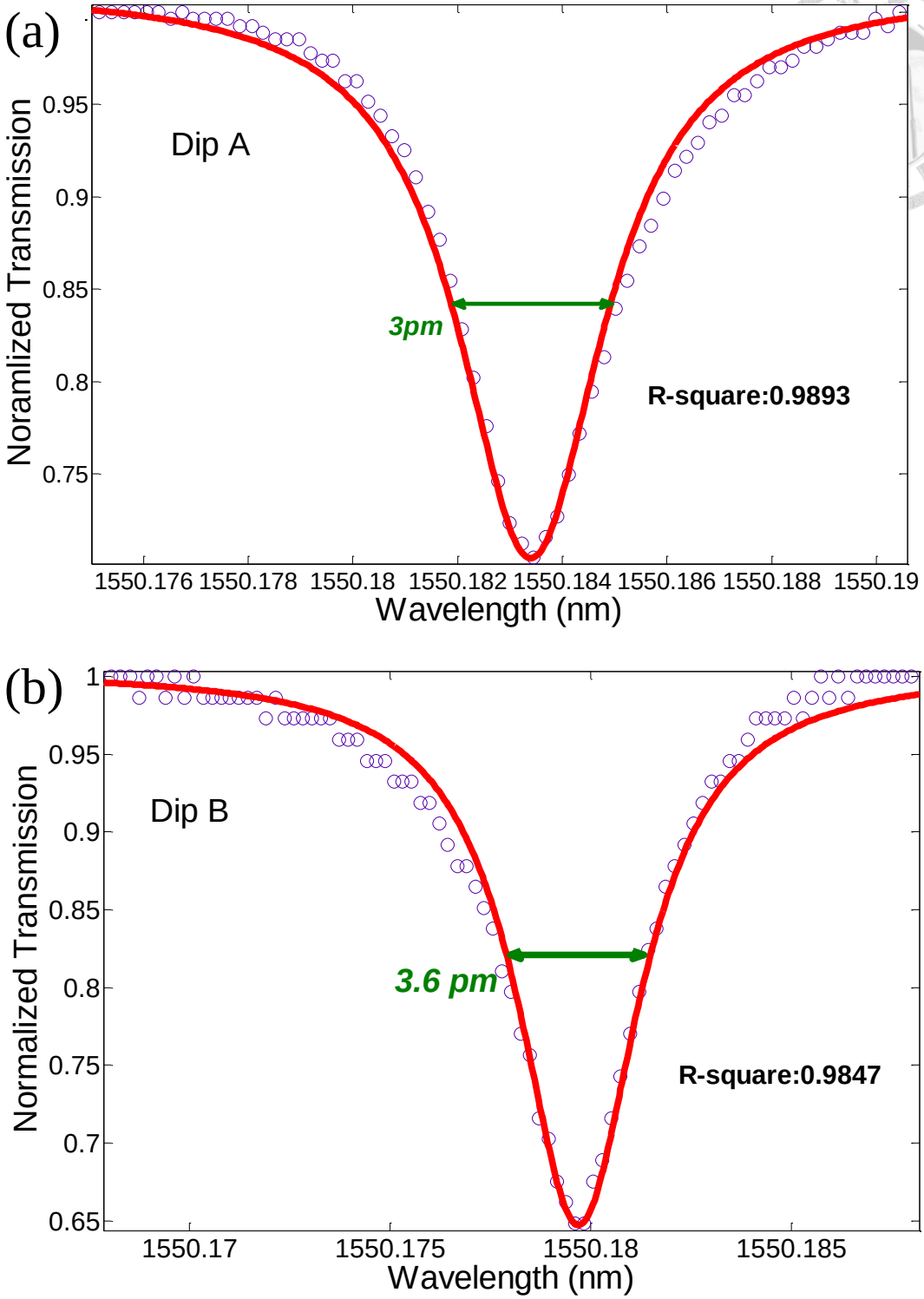

Fig. 3-13 Lorentz curve fittings of (a) dip A and (b) dip B.

doi:10.6342/NTU201700769

3.3 Long-term Stability Improvement

Microfiber coil resonator have been studied for many applications in nonlinear optics, optical sensing and communication. For practical applications, stable performance is needed. The MCR part has been packaged by PDMS, while some microfibers are without protection. As mentioned before, microfiber is easily affected by surrounding disturbance. Therefore, protection method for microfiber is essential to ensure stable performance.

After the fabrication process described in Chapter 2, the PDMS-packaged MCR was taken from coiling system carefully and fixed on a clip. Then the MCR was moved to a U-shape Aluminum holder with two clips, as shown in Fig. 3-14. The U-shaped holder was designed to support the whole MCR structure in the following process. If the microfibers were adhered to one another during this step, a segment of glass fiber was used to separate them. The microfibers should be as straight as possible so that they would not adhere again. The single mode fiber region was taped on U-shaped holder. After the whole structure was fixed, the U-shaped holder was screwed to the package system. Fig. 3-15 shows the package system. The package system includes two manual z-axis stages, a manual xy-axis stage and a tilt stage.

A PMMA board coated with UV glue (PC373L AP, Luvantix SSCP, n~1.373) was

doi:10.6342/NTU201700769

used as low refractive index substrate for PDMS-packaged MCR. It was noticed that the surface of UV glue coating would be sticky due to oxygen inhibition. Oxygen inhibition is resulted from the oxygen in air. During the UV curing process, oxygen interacts with photoninitiator by quenching effect. Besides, oxygen can react with radicals produced from photoninitiator. Both would slow reaction rate and lead to low degree of curing [49]. The sticky surface might adhere microfibers and break microfibers in the following process. To solve this problem, a polyethylene (PE) thin film was covered on the UV glue coating during the curing process. The PE thin film could isolate the UV glue from oxygen so that the coating could be fully cured.

Now we describe the package process. The PMMA board with UV glue coating was set on a manual z-axis stage. The U-shaped holder with PDMS-packaged MCR was screwed to the tilt stage. The position of PDSM-packaged MCR was moved right above the PMMA board by adjusting manual xy-axis stage. Then the PMMA board was raised to support the PDMS-packaged MCR. Tilt stage was used to make microfibers parallel with PMMA board so that the microfibers could touch PMMA board without bending. Finally, the microfibers was covered with enough UV glue and exposed by UV LED for 10 minutes. As mentioned before, a PE thin film was covered on UV glue to prevent oxygen inhibition. Here PDMS was not appropriate to package microfibers. It was hard to stretch the microfibers straight on U-shaped holder, so microfibers were

doi:10.6342/NTU201700769

a little loose. Since the thermal expansion coefficient of PDMS is larger than silica [50, 51], PDMS would compress microfibers during thermal curing process. As shown in Fig. 3-16, these micro-bending would increase propagation loss to microfibers. In our previous test, the transmission power of microfiber would be down to zero when micro-bending happened.

Fig. 3-17 shows the photograph of the whole structure. The measured transmission spectrum is shown in Fig. 3-18 (a). The free spectral range was 0.283 nm, and the extinction ratio was ~4.5 dB. Lorentzian curve fitting was applied to determine the bandwidth of dip. As seen in Fig. 3-18 (b), the bandwidth of the resonant dip at 1549.941 nm was 16 pm and the quality factor ($\lambda/\Delta\lambda$) was ~100,000. Fig. 3-19 shows the original transmission spectrum and the spectrum after a month. The transmission power level and shape of resonant dip almost remained unchanged. This result showed that packaging microfibers with UV glue could improve the long-term stability of PDMS-packaged MCR.

doi:10.6342/NTU201700769

Fig. 3-14 Photograph of U-shaped Aluminum and MCR clip.

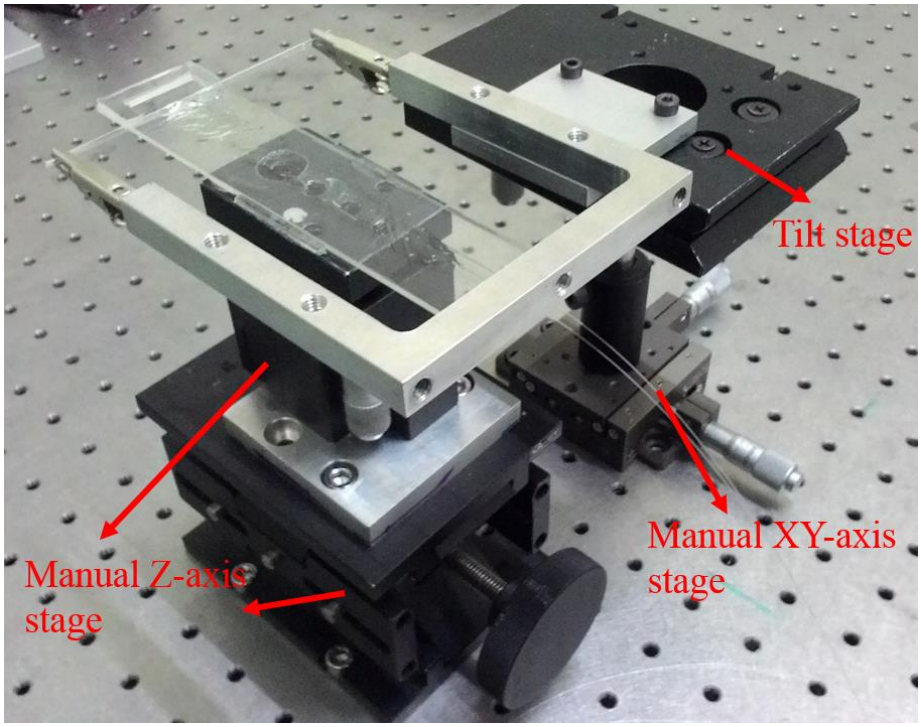

Fig. 3-15 Photograph of package system.

doi:10.6342/NTU201700769

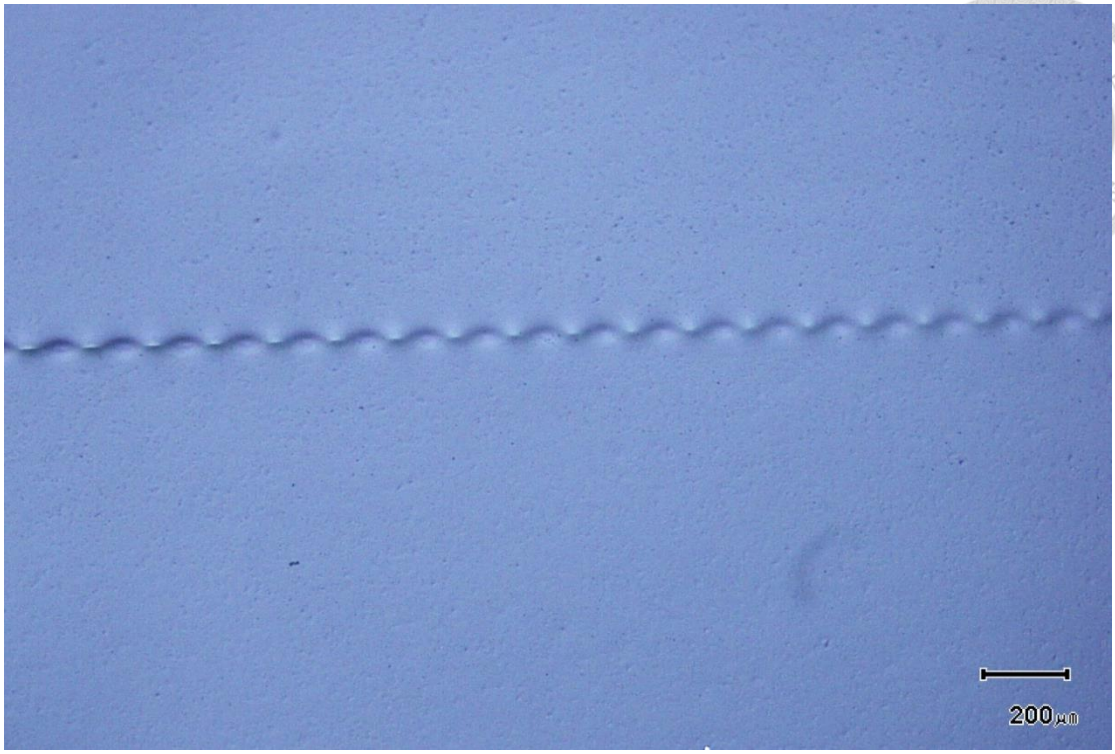

Fig. 3-16 Photograph of microfiber in PDMS with micro-bending.

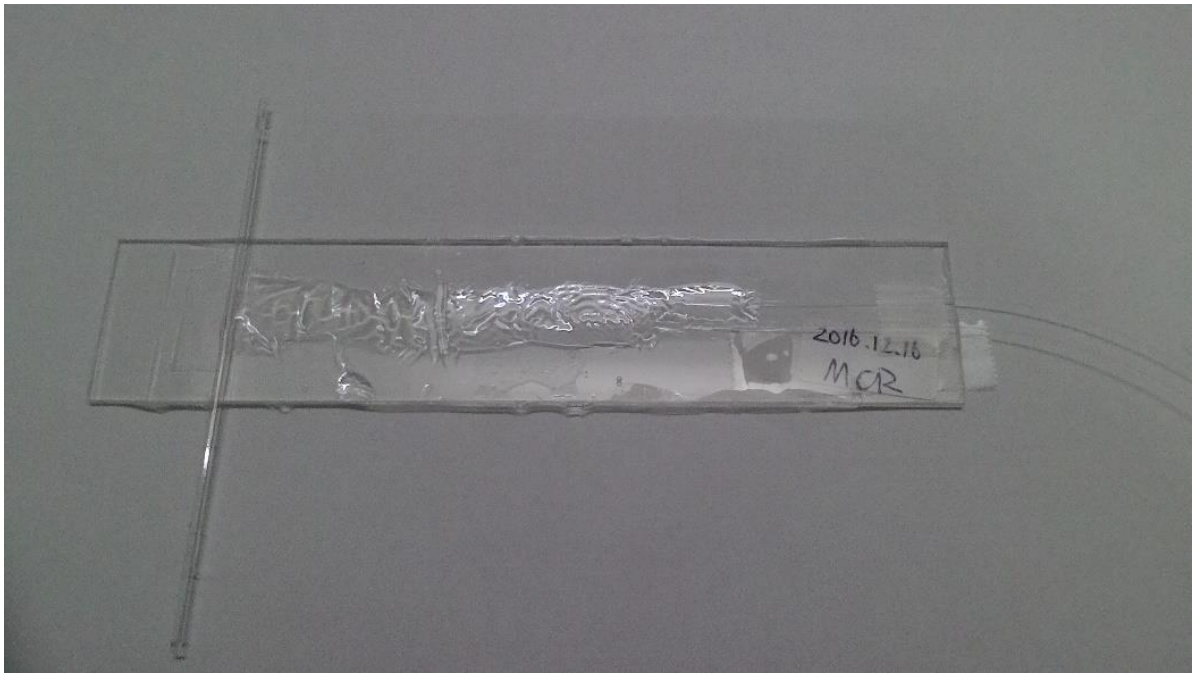

Fig. 3-17 Photograph of PDMS-packaged MCR on UV glue coating substrate.

doi:10.6342/NTU201700769

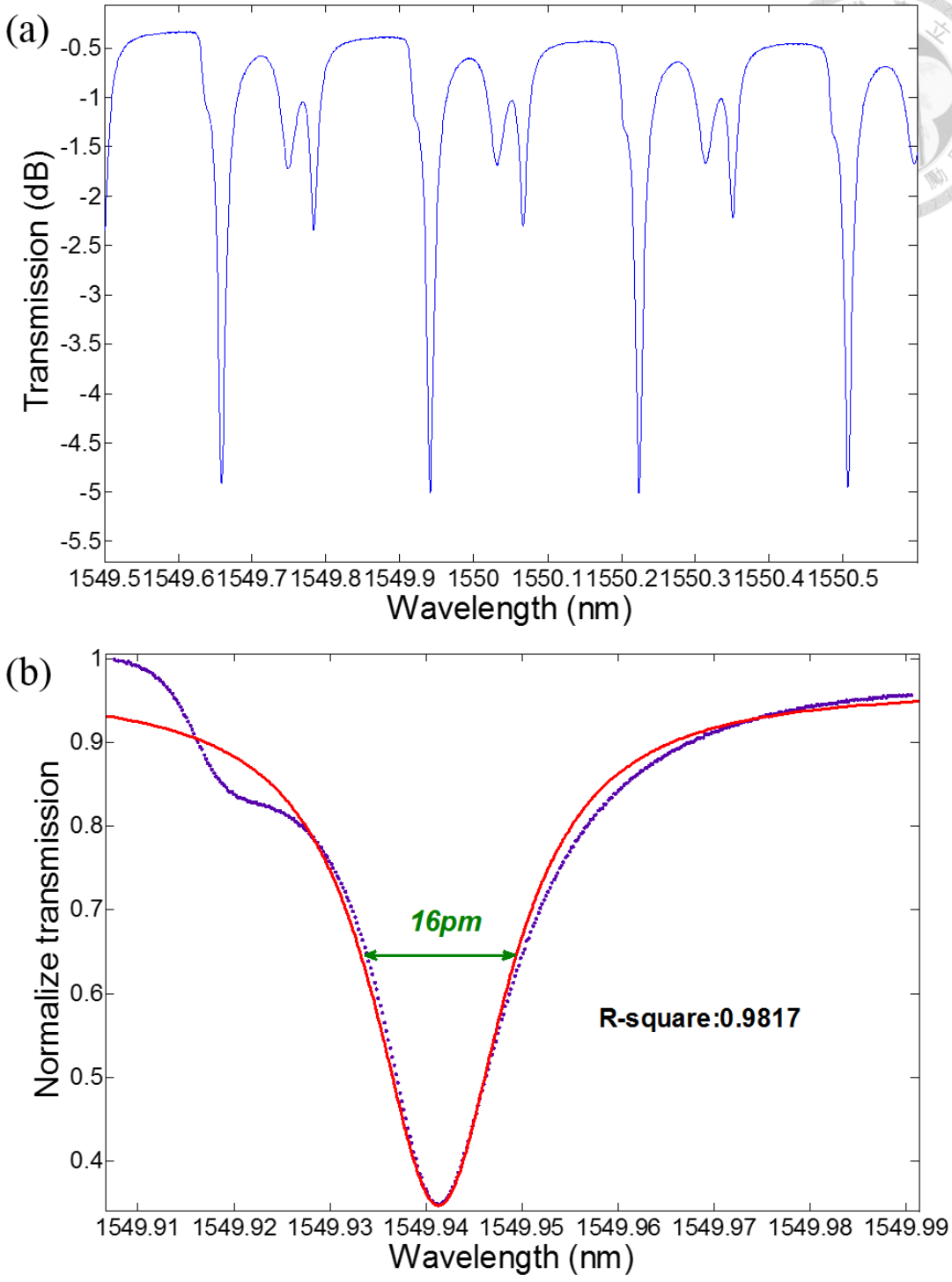

Fig. 3-18 (a) Transmission spectrum of PDMS-packaged MCR and (b) one resonant dip and its Lorentz curve fitting

doi:10.6342/NTU201700769

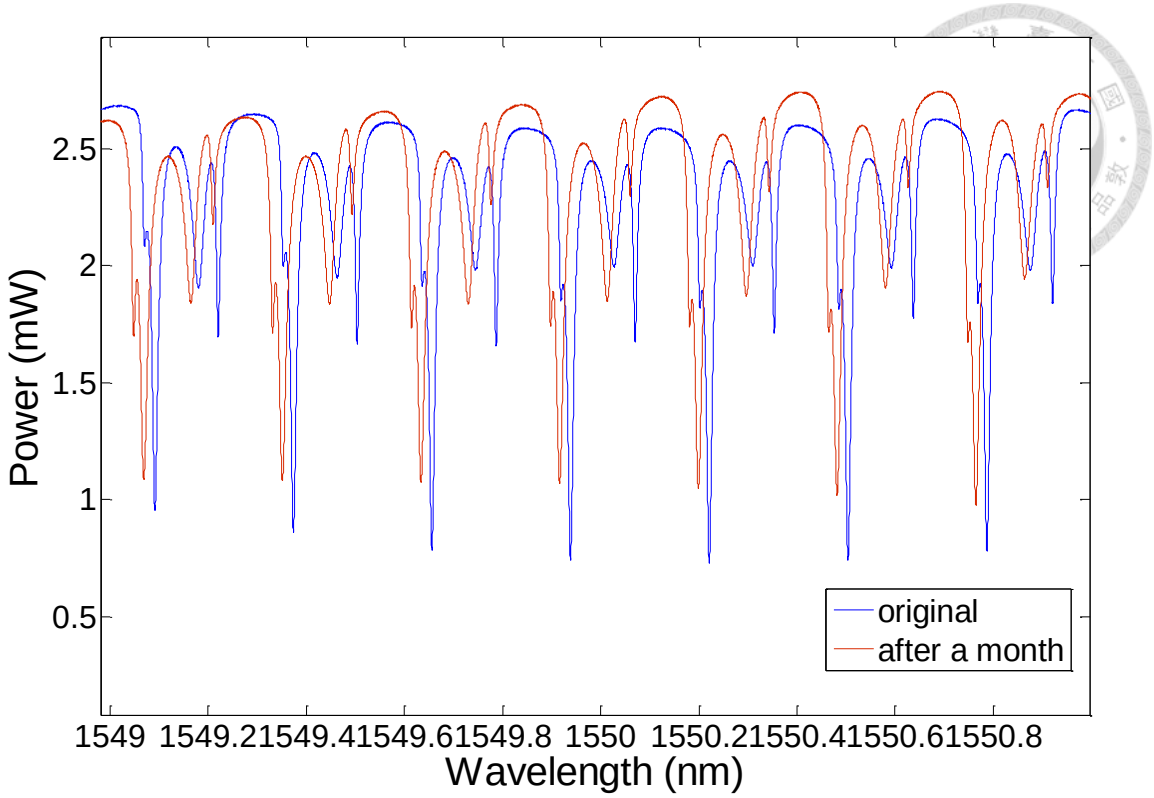

Fig. 3-19 Transmission spectra of the original PDMS-packaged MCR with protection and the same one after a month.

doi:10.6342/NTU201700769

Chapter 4 Conclusions and Future Work

In this work, a PDMS-packaged MCR with high quality factor has been demonstrated. PDMS for packaging MCR was diluted with hexane so the MCR coil could turn around easily. The quality factor was 5 x 10^5 and the performance could maintain for 5 days. With high quality factor and a stable MCR structure, PDMS-packaged MCR could serve as RI sensor with low detection limit. A 4-layer PMMA structure was designed to support PDMS-packaged MCR and glucose solutions were used for different RI. The experiment results showed the resonance dips shifted linearly and the detection limit was 7 x 10^{-4}. To increase the potential of practical applications, long-term stability of MCR was further improved by protecting microfibers with UV glue. In UV curing process, UV glue was covered with PE thin film to prevent oxygen inhibition. The performance of MCR could maintain over a month without degradation. Such MCRs with high quality factor and long-term stability might be useful in nonlinear optics.

When an optical fiber is drawn into a microfiber, the nonlinear interaction occurs in the narrow microfiber waist. Microfiber allows light to be funneled into a small area, increasing its intensity and promoting nonlinear effect. Besides, a resonator with high quality is usually along with enhanced nonlinearity due to strong optical confinement.

doi:10.6342/NTU201700769

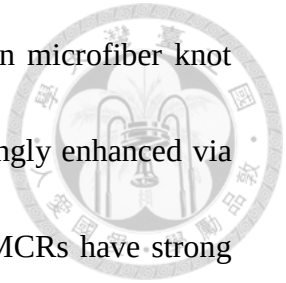

In 2015, Y. Wang *et. al.*, presented an all optical control based on microfiber knot resonator and graphene. The light-graphene interaction can be strongly enhanced via the resonantly circulating light [52]. Therefore, PDMS-packaged MCRs have strong nonlinearity and can provide a stable structure for nonlinear optics. Recently, the combination of semiconductor materials with fiber optics has become one of the emerging research topics. We have the ability to produce silicon-cored fibers with high quality by vertical-drawing [53]. The nonlinear effect of silicon is stronger than silica. We can fabricate PDMS-packaged MCR with microfiber drawn from silicon-cored fiber. PDMS-packaged MCR combined with silicon-cored fiber would have strong nonlinear effect and potential for nonlinear applications.

In addition to the nonlinear application, MCRs with high quality factor have the potential to be good lasing element. In 2006, X. Jiang *et. al.*, demonstrated a microfiber laser formed by tightening a doped microfiber into a microfiber knot resonator [54]. With high quality factor and long-term stability, PDMS-packaged MCR could supply good condition for lasing. We could draw the fiber with high gain doping into microfiber and use the microfiber to fabricate PDMS-packaged MCR. The MCR based laser is likely to be realized.

doi:10.6342/NTU201700769

References

[1] K. C. Kao and G. A. Hockham, "Dielectric-fibre surface waveguides for optical frequencies," IEE Proc. J., vol. 113, pp. 1151–1158, 1966.

[2] Senior, John M., and M. Yousif Jamro. *Optical Fiber Communications: Principles and Practice*. Pearson Education, 2009.

[3] P. Urquhart, "Review of rare earth doped fibre lasers and amplifiers," IEE Proceedings J. Optoelectronics, vol. 135, pp. 385-407, 1988.

[4] R. Kashyap, *Fiber Bragg Gratings*. Academic Press, 2009.

[5] Rajan Ginu, ed. *Optical Fiber Sensors: Advanced Techniques and Applications*. CRC press, 2015.

[6] R. H. Stolen and R. P. De Paula, "Single-mode fiber components," Proc. IEEE, vol. 75, pp. 1498–1511, 1987.

[7] J.-P. Goure, I. Verrier, and J.-P. Meunier, "Linear and nonlinear optical fibre devices," J. Phys. D-Appl. Phys., vol. 22, pp. 1791–1805, 1989.

[8] P. Matthijsse and W. Griffioen, "Matching optical fiber lifetime and bend-loss limits for optimized local loop fiber storage," Opt. Fiber Technol., vol. 11, pp. 92–99, 2005.

[9] P. Wang, Q. Wang, G. Farrell, G. Rajan, T. Freir, and J. Cassidy, "Investigation

doi:10.6342/NTU201700769

of macrobending losses of standard single mode fiber with small bend radii," Microw. Opt. Technol. Lett., vol. 49, pp. 2133–2138, 2007.

[10] N. G. R. Broderick, "Optical Snakes and Ladders: Dispersion and nonlinearity in microcoil resonators," Opt Express, vol. 16, pp. 16247-16254, 2008.

[11] G. Brambilla, "Optical fibre nanotaper sensors," Opt. Fiber Technol, vol. 16, pp. 331-342, 2010.

[12] J. Scheuer, "Fiber microcoil optical gyroscope," Opt. Lett., vol. 34, pp. 1630-1632, 2009.

[13] F. Xu, P. Horak, and G. Brambilla, "Optical microfiber coil resonator refractometric sensor," Opt. Express, vol. 15, pp. 7888-7893, 2007.

[14] Y. C. Hsieh, T. S. Peng, and L. A. Wang, “Millimeter-Sized Microfiber Coil Resonators with Enhanced Quality Factors by Increasing Coil Numbers,” IEEE Photon. Technol. Lett., 24, pp. 569-571, 2012

[15] T. H. Shen and L. A. Wang, “A Two-Layer Microcoil Resonator with Very High Quality Factor,” IEEE Photon. Technol. Lett., 26, pp. 535-537, 2014.

[16] F. Xu and G. Brambilla, “Embedding optical microfiber coil resonators in Teflon,” Opt. Lett. 32, pp. 2164-2166, 2007.

[17] Y. Jung, G. S. Murugan, G. Brambilla, and D. J. Richardson, “Embedded optical microfiber coil resonator with enhanced high-Q,” IEEE Photon.

doi:10.6342/NTU201700769

Technol. Lett., 22, pp. 1638–1640, 2010.

[18] L. Tong and M. Sumetsky, *Subwavelength and Nanometer Diameter Optical Fibers*. Springer, 2010.

[19] G. Brambilla, F. Xu, P. Horak, Y. Jung, F. Koizumi, N. P. Sessions, E. Koukharenko, X. Feng, G. S. Murugan, J. S. Wilkinson, and D. J. Richardson, "Optical fiber nanowires and microwires: Fabrication and applications," Adv. Opt. Photon., vol. 1, pp. 107–161, 2009.

[20] G. Brambilla, "Optical fibre nanowires and microwires: A review," J. Optics., vol. 12, pp. 043001, 2010.

[21] J. Scheuer and M. Sumetsky, "Optical - fiber microcoil waveguides and resonators and their applications for interferometry and sensing," Laser Photon. Rev., vol. 5, pp. 465–478, 2011.

[22] F. Xu and G. Brambilla. "Demonstration of a refractometric sensor based on optical microfiber coil resonator," Appl. Phys. Lett., vol. 92, pp. 101126, 2008.

[23] G. Xin and L. Tong. "Supported microfiber loops for optical sensing." Opt. Express, vol. 16, pp. 14429-14434, 2008.

[24] K.S. Lim, I. Aryanfar, W.Y. Chong, Y.K. Cheong, S.W. Harun, and H. Ahmad, "Integrated microfibre device for refractive index and temperature sensing," Sensors, vol. 12, pp. 11782-11789, 2012.

doi:10.6342/NTU201700769

[25] H. Yu, L. Xiong, Z. Chen, Q. Li, X. Yi, Y. Ding, F. Wang, H. Lv, and Y. Ding, "Solution concentration and refractive index sensing based on polymer microfiber knot resonator," Appl. Phys. Express, vol.7, pp. 022501, 2014.

[26] X. Li and H. Ding, "A stable evanescent field-based microfiber knot resonator refractive index sensor." IEEE Photon. Technol. Lett, vol. 26, pp. 1625-1628, 2014.

[27] X. Zeng, Y. Wu, C. Hou, J. Bai and G. Yang, "A temperature sensor based on optical microfiber knot resonator," Optics Communications, vol. 282, pp. 3817-3819, 2009.

[28] K.S. Lim, S.W. Harun, S.S.A. Damanhuri, A.A. Jasim, C.K. Tio and H. Ahmad, "Current sensor based on microfiber knot resonator," Sensors and Actuators A: Physical, vol. 167, pp. 60-62, 2011.

[29] X. Xie, J. Li, L.P. Sun, X. Shen, L. Jin and B.O. Guan, "A high-sensitivity current sensor utilizing CrNi wire and microfiber coils," Sensors, vol. 14, pp. 8423-8429, 2014.

[30] S.C. Yan, B.C. Zheng, J.H. Chen, F. Xu and Y.Q. Lu, (2015). "Optical electrical current sensor utilizing a graphene-microfiber-integrated coil resonator," Appl. Phys. Lett., vol. 107, pp. 053502, 2015.

[31] M.S. Yoon, S.K. Kim and Y.G. Han, "Highly sensitive current sensor based on

doi:10.6342/NTU201700769

an optical microfiber loop resonator incorporating low index polymer overlay," J. Lightw. Technol., vol. 33, pp. 2386-2391, 2015.

[32] Y. Wu, T. Zhang, Y. Rao and Y. Gong, "Miniature interferometric humidity sensors based on silica/polymer microfiber knot resonators." Sensors and Actuators B: Chemical, vol. 155, pp. 258-263, 2011.

[33] P. Wang, F. Gu, L. Zhang and L. Tong, "Polymer microfiber rings for high-sensitivity optical humidity sensing." Applied Optics, vol. 50, pp. G7-G10, 2011.

[34] M.A. Gouveia, P.E. Pellegrini, J.S. dos Santos, I.M. Raimundo and C.M. Cordeiro, "Analysis of immersed silica optical microfiber knot resonator and its application as a moisture sensor." Applied Optics, vol. 53, pp. 7454-7461, 2014.

[35] Y.S. Chiam, K.S. Lim, S.W. Harun, S.N. Gan and S.W Phang, "Conducting polymer coated optical microfiber sensor for alcohol detection." Sensors and Actuators A: Physical, vol.205, pp. 58-62, 2014.

[36] X. Wu, F. Gu and H. Zeng, "Palladium-coated silica microfiber knots for enhanced hydrogen sensing." IEEE Photon. Technol. Lett.,vol. 27, pp. 1228-1231, 2015.

[37] X. Li and H. Ding, "Temperature insensitive magnetic field sensor based on

doi:10.6342/NTU201700769

ferrofluid clad microfiber resonator." IEEE Photon. Technol. Lett., vol. 26, pp. 2426-2429, 2014.

[38] X. Li and H. Ding, "All-fiber magnetic-field sensor based on microfiber knot resonator and magnetic fluid." Optics Letters, vol. 37, pp. 5187-5189, 2012.

[39] L. Xiao, M.D.W. Grogan, S.G. Leon-Saval, R. Williams, R. England, W.J. Wadsworth and T.A. Birks, "Tapered fibers embedded in silica aerogel." Optics Letters, vol. 34, pp. 2724-2726, 2009.

[40] I. Hernández-Romano, D. Monzón-Hernández, C. Moreno-Hernández, D. Moreno-Hernandez and J. Villatoro "Highly sensitive temperature sensor based on a polymer-coated microfiber interferometer." IEEE Photon. Technol. Lett., vol. 27, pp. 2591-2594, 2015.

[41] X. Zhang, M. Belal, G. Y. Chen, Z. Song, G. Brambilla, and T. P. Newson, "Compact optical microfiber phase modulator," Optics Letters, vol. 37, pp. 320–322, 2012.

[42] A. W. Snyder, "Coupled-Mode Theory for Optical Fibers," Journal of the Optical Society of America, vol. 62, pp. 1267-1277, 1972.

[43] M. Sumetsky, "Optical fiber microcoil resonator," Opt. Express, vol. 12, pp. 2303-2316, 2004.

[44] M. L. Gorodetsky, A. D. Pryamikov, and V. S. Ilchenko, "Rayleigh scattering

doi:10.6342/NTU201700769

in high-Q microspheres," Journal of the Optical Society of America B-Optical Physics, vol. 17, pp. 1051-1057, 2000.

[45] T. H. Shen, Fabrication of Two-layer Microcoil Resonators with Very High Quality Factors by Using Ultra-low Porpagation Loss Microfibers, in Graduate Institute of Photonics and Optoelectronics2013, National Taiwan University: Taipei.

[46] J.N. Lee, C. Park and George M. Whitesides. "Solvent compatibility of poly (dimethylsiloxane)-based microfluidic devices." Analytical Chemistry, vol. 75, pp. 6544-6554, 2003.

[47] C. Y. Chao and L. J. Guo, "Design and optimization of microring resonators in biochemical sensing applications," Journal of Lightwave Technology, vol. 24, pp. 1395-1402, 2006.

[48] R. Lorenzi, Y. Jung, and G. Brambilla, "In-line absorption sensor based on coiled optical microfiber." Appl. Phys. Lett., vol. 98, pp. 173504, 2011.

[49] C. Bentivoglio Ruiz, L. Machado, J. Volponi and E. Segura Pino, "Oxygen inhibition and coating thickness effects on UV radiation curing of weatherfast clearcoats studied by photo-DSC." Journal of Thermal Analysis and Calorimetry, vol. 75, pp. 507-512, 2004.

[50] Q. Wang, C. Du, J. Zhang, R. Lv and Y. Zhao, "Sensitivity-enhanced

doi:10.6342/NTU201700769

temperature sensor based on PDMS-coated long period fiber grating." Optics Communications, vol. 377, pp. 89-93, 2016.

[51] C.S. Park, K.I. Joo, S.W. Kang and H.R. Kim, "A PDMS-coated optical fiber Bragg grating sensor for enhancing temperature sensitivity." Journal of the Optical Society of Korea, vol. 15, pp. 329-334, 2011.

[52] Y. Wang, X. Gan, C. Zhao, L. Fang, D. Mao, Y. Xu, F. Zhang, T. Xi, L. Ren and J. Zhao, "All-optical control of microfiber resonator by graphene's photothermal effect." Appl. Phys. Lett., vol.108, pp. 171905, 2016

[53] Y. B. Huang, Fabrication of Schottky photodetector by using Si-cored fibers, in Graduate Institute of Photonics and Optoelectronics2015, National Taiwan University: Taipei.

[54] X. Jiang, Q. Yang, G. Vienne, Y. Li, L. Tong, J. Zhang and L. Hu, "Demonstration of microfiber knot laser." Appl. Phys. Lett., vol. 89, pp. 143513, 2006.

doi:10.6342/NTU201700769